2015

Mathematical Model of the Split Firefly Luciferase Assay

Renee Dale
Louisiana State University and Agricultural and Mechanical College

MATHEMATICAL MODEL OF THE SPLIT FIREFLY LUCIFERASE ASSAY

A Thesis

Submitted to the Graduate Faculty of the
Louisiana State University and
Agricultural and Mechanical College
in partial fulfillment of the
requirements for the degree of
Masters of Science

in

The Department of Biological Sciences

by
Renee Dale
B.S., B.A., Louisiana State University, 2013
August 2015

Acknowledgments

I would like to thank my professor, Dr. Kato, and my committee members, Dr. Waldrop and Dr. He. I would also like to thank our collaborators, Dr. Ohmuro-Matsuyama, and Dr. Ueda.

Table of Contents

List of Tables

List of Figures

Abstract

The firefly luciferase complementation assay is widely used as a bioluminescent reporter technology to detect protein-protein interactions *in vitro* and *in vivo*. Firefly luciferase oxidates its substrate, luciferin, resulting in the emission of light. A previous study suggests that the firefly luciferase complementation assay has different luminescence kinetics from full length luciferase. The mechanism behind this is still unknown. Although half of the previously published studies utilizing the firefly luciferase complementation assay consider it quantitative. To understand how the molecular reactions and the changes in the affinity of the protein pair affect experimental results, a mathematical model was constructed. This suggests that previously published studies should be considered qualitative, unless an additional experiment is performed. This new model demonstrates that the luminescence measured is not linearly correlated with the affinity of the protein pair. The model is then used to design a new experiment which allows the firefly luciferase complementation assay to be used quantitatively to detect changes of affinity.

Chapter 1
Introduction

1.1 The firefly luciferase complementation assay

The firefly luciferase complementation assay (FLCA) is an assay that detects protein-protein interactions *in vitro* as well as *in vivo* both at the cellular and organismal level [68, 23]. The assay detects the bioluminescence that is emitted during the oxidation of the substrate, D-Luciferin (LH_2). In the assay, the N-terminal and C-terminal domain of firefly luciferase (NFLuc and CFLuc, respectively) are genetically fused to a protein pair of interest ([88]). When the protein pair interacts luminescence is observed.

The FLCA can be used in many systems. In the *in vitro* assays previously conducted [28], the substrates LH_2 and ATP are added to a 96-well plate containing the enzyme. Luminescence is measured in relative units (RLU) as photomutlipler tubes are used to detect photons. In the *in vivo* assay, the cells of interest are suspended in the 96-well plate. LH_2 is brought into contact with the enzyme via diffusion through the cell membranes. When performing FLCA in a live mouse, LH_2 is injected into a tail vein [42]. The typical luminescence kinetics of firefly luciferase include a peak within a few seconds followed by a gradual decay, although the FLCA kinetics have a slower peak and decay [12, 28]. The maximum relative luminesence (RLU) is generally used to evaluate the interaction of the protein pair.

1.1.1 Problems with experimental interpretation

Although the FLCA is valued for simplicity of the assay, it is not a simple system from a enzymatic reaction point of view (Fig. 1.1). While NFLuc alone has residual enzymatic activity (binding and catalysis of the substrates), the C domain is key in increasing the efficiency of the catalytic steps [38, 3, 6, 8]. Hence in the FLCA, the affinity of a protein pair of interest fused to NFLuc or CFLuc should influence the luminescence output by altering the interaction between NFLuc and CFLuc.

Bioluminescent complementation assays have the advantage of being usable *in vivo* without disrupting the cell's environment [88]. The firefly luciferase complementation assay was designed to be a bioluminesent reporter technology *in vivo*. To establish it as a viable technique, it was determined that NFLuc alone created low enough luminesence to be considered background *in vivo* [88]. Western blotting was used to show that the enzyme is being reconstituted upon the interaction of the proteins fused to NFLuc and CFLuc. It was also found that the FLCA could detect protein interactions in human embryonic kidney cells (HEK) and in living mice [88].

Disagreement on the interpretation of FLCA data The interpretation of previously published FLCA data ranges from the presence or absence of protein interactions to quantitative measurement of the protein interaction (i.e. [41] to [87]). Some of the previously published articles claim that the maximum RLU detected during the assay is quantitative

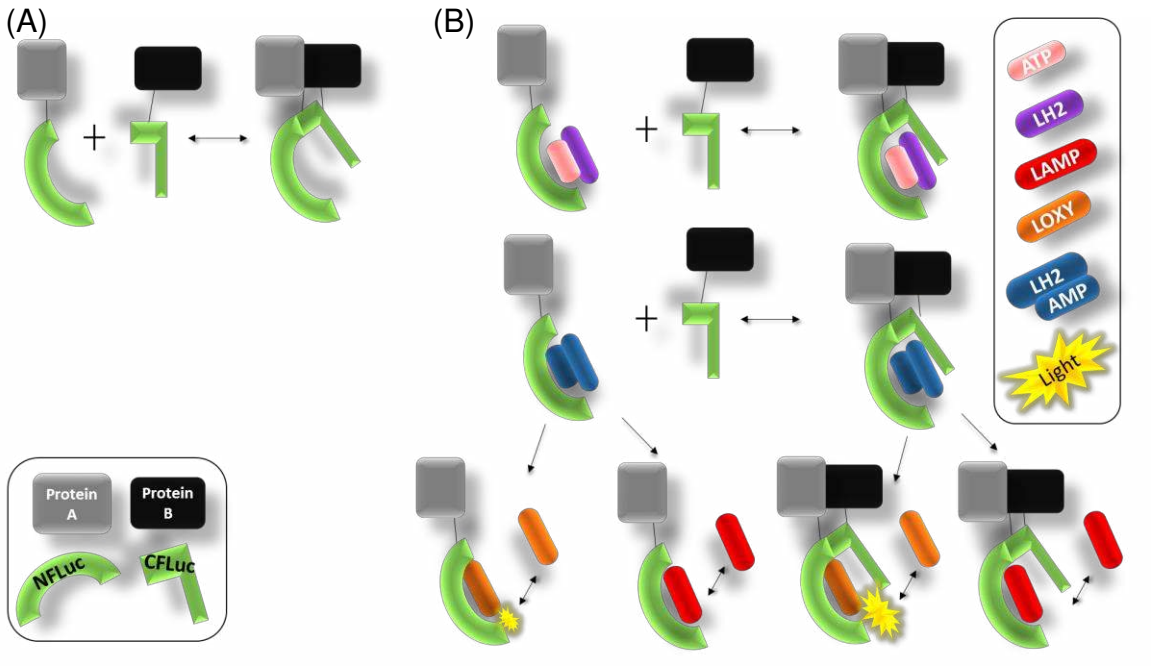

Figure 1.1: Overview of *in vitro* firefly Luciferase complementation assay (FLCA) system. (A) With interaction of the protein pair, the N and C domains of luciferase (NFLuc and CFLuc, respectively) reconstitute the active site of the enzyme. The amount of NC complex is correlated with the affinities of the protein pair in question. (B) Upon the addition of the substrates, LH_2 and ATP, catalysis occurs in a two step process. The enzyme first adenylates the substrates LH_2 and ATP, forming the intermediate LH_2-AMP. The intermediate is then oxidized to form L-oxyluciferin (L-oxy) during the light emission reaction. Alternatively, the intermediate is oxidized to form dehydroluciferyl-AMP (L-AMP) without emitting light. Both products inhibit luciferase competitively. NFLuc has small amounts of activity on its own [38, 3].

because the maximum RLU depends upon the presence of interaction between proteins and the amount of proteins present [21]. From 46 previously published articles using the FLCA, 49% interpreted the data quantitatively (i.e. [41] to [87]). In such articles, FLCA data are considered quantitative because of an assumption that the reconstituted activity of split firefly luciferase is entirely and linearly dependent upon the amount of a protein pair interacting with each other, which in turn is dependent upon the affinity.

In Chen et al, 9 pairs of proteins known to interact in plants were fused to NFLuc or CFLuc and the FLCA was performed *in vivo* [41]. Bacterial effector proteins from *Pseudomonas syringae* were used as bait, and their various protein targets as prey proteins. Their protein targets included proteins involved in the E3 ligase complex, chaperone complex, disease resistance, and transcription factors. They also mutated the protein targets of the effector proteins to serve as negative controls for the interaction. High luminescence was observed for the positive interaction pairs, whereas low luminescence for the control pairs. From this, they concluded that if the amount of interacting bait and prey proteins could be

quantified using a Western blot, the affinity of the interacting proteins could be deduced from the RLU.

Another paper had a similar conclusion. In Li et al, 12 AUX/IAA proteins (plant hormone binding proteins) were fused to NFLuc as the bait. The prey consisted of 8 carboxy-terminal domains of ARF proteins (plant transcription factors) which were fused to CFLuc [51]. The carboxy-terminal domain of ARF is known to dimerize with AUX/IAA proteins, although it was unknown which of the 12 proteins it would interact with *in vivo*. They found high variation in the observed luminescence, and performed co-immuno precipitation to find relative concentrations of NFLuc bound to CFLuc for some protein pairs. They found a linear relationship between amount of NFLuc bound to CFLuc, and concluded the luminescence is linearly correlated with the affinity of the protein pair.

However, a relationship between changes of the affinity of the protein pair and the luminescence detected in the FLCA has not been quantitatively understood. In fact, it has been shown previously that the kinetics of luminescence production in the FLCA is very different from that in full length firefly luciferase [3, 38, 21]. Without a thorough understanding of the cause for these changes in the luminescence kinetics, or a demonstration of a linear relationship between protein interaction and luminescence, the FLCA cannot reasonably be considered quantitative. The purpose of this thesis is to quantitatively understand the relationship between changes of the affinity of a protein pair and the luminescence detected in the FLCA using a mathematical model. The model is built upon the known enzymatic reactions and the equilibrium constants identified for both firefly luciferase and the protein pair. Using the model, quantitative or qualitative nature of FLCA data will be analyzed.

1.2 The firefly luciferase reaction

1.2.1 Structure of firefly luciferase

Firefly luciferase is a 62 kDa oxygenase encoded by 550 amino acids [9]. X-ray crystallography has revealed that the N domain is encoded in amino acids 4-436, and the C domain in amino acids 440-544 [9]. There is a flexible hinge region between the two domains at amino acids 436-440 [9]. The flexible linker region allows the C domain to change conformation during the oxidation step, allowing the catalytic residue to come in contact with the substrate (Fig. 1.2). Both of the primary amino acids involved in catalysis are on the C domain. Amino acid K429 is responsible for adenylation, while K443 oxidizes the substrates [8, 6]. Gene mutation studies identified binding sites for LH_2 and ATP encoded in amino acids 213-348 of the N domain [7]. N domain residue H245 is considered the key binding residue, as it is highly conserved throughout the adenylase family in addition to being in the region identified as responsible for binding of substrates [7]. The firefly luciferase complementation assay design consists of the enzyme split into two portions, the N and C domains. NFLuc consists of amino acids 1-437, and CFLuc contains 395-547 [28]. The overlapping region common to both NFLuc and CFLuc, amino acids 395-437, includes the flexible linker region and part of the N domain.

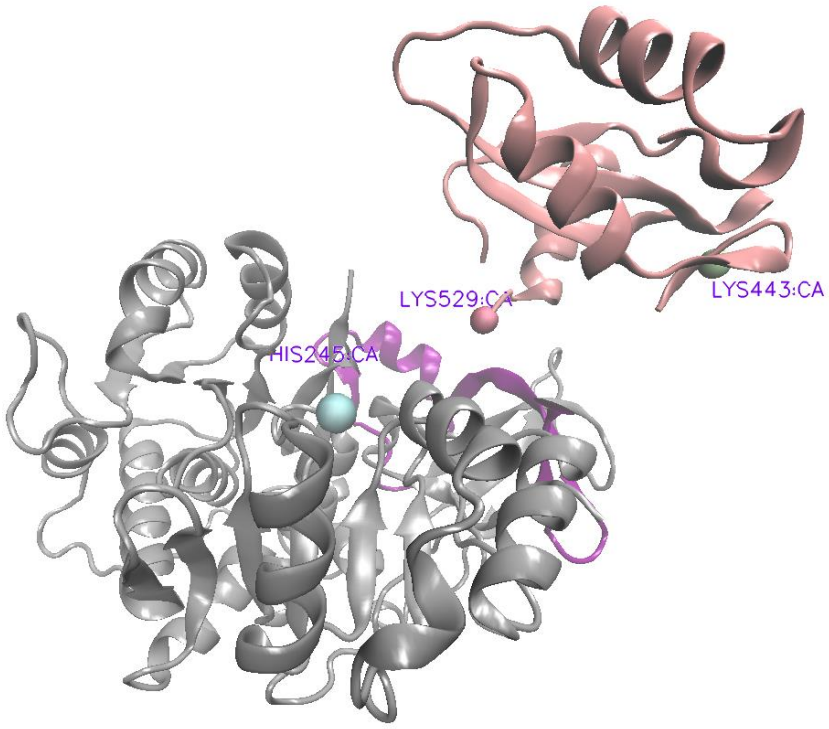

Figure 1.2: The key residues of the N domain (grey and purple) and the C domain (pink). When firefly luciferase is split, part of the enzyme is common to both NFLuc and CFLuc (purple). This region primarily consists of the flexible linker region between the N and C terminal domains of firefly luciferase. As indicated here, the C domain and CFLuc contains the key residues for adenylation (red, K529) and oxidation (green, K443), while the N domain and NFLuc contains the key binding residue (blue, H245). Image generated using Visual Molecular Dynamics (VMD) software with the crystal structure of luciferase solved by Conti et al [15, 9].

1.2.2 Mechanism of Luminesence

The molecular mechanism of full length firefly luciferase reaction has been well established [19, 11, 25, 89]. During adenylation step, ATP and LH_2 are adenylated to form the intermediate luciferyl-adenylate (LH_2-AMP) (Reaction 1.1). The oxygen on the carboxyl group of LH_2 acts as a nucleophile (Fig. 1.2.2), and the α phosphorous of ATP acts as an electrophile [25]. Mg^{2+} is utilized by ATP to shield the negative charges and aid in the electrophilic action of the phosphorous. AMP is transferred to LH_2, forming the intermediate, LH_2-AMP, and pyrophosphate leaves. Luciferase then oxidizes this intermediate via the following generally accepted mechanism [6]. Lysine 529 removes a proton from the C_4 carbon, creating a carbanion. O_2 is then added to the carbanion, forming a dioxetanone after AMP leaves. The instability of the dioxetanone causes it to spontaneously generate CO_2 (Reaction 1.2). This creates oxyluciferin in a singlet excited state. As oxyluciferin decays to its ground state, it releases a photon and luminesence is observed (Reaction 1.3). The quantum yield of firefly luciferase is approximately one photon released per excited oxyluciferin [9].

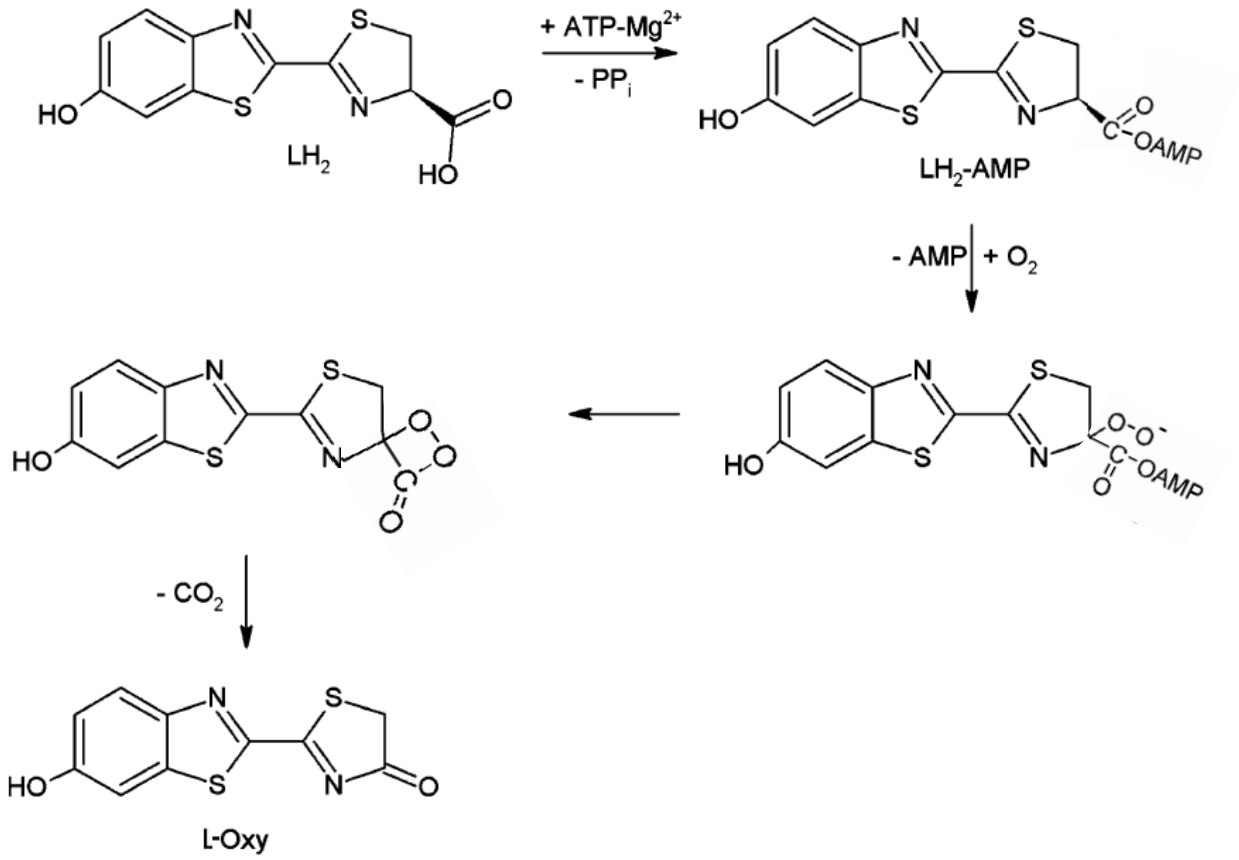

Figure 1.3: The chemical reactions catalyzed by firefly luciferase. Firefly luciferase adenylates LH_2 to form the intermediate, LH_2-AMP. O_2 is added to the intermediate, forming an unstable dioxetanone. The dioxetanone spontaneously generates CO_2 and L-oxyluciferin.

$$\text{Luc} + LH_2 + \text{ATP} \overset{Mg^{2+}}{\rightleftharpoons} \text{Luc} \cdot LH_2\text{–AMP} + PP_i \quad \{1.1\}$$

$$\text{Luc} \cdot LH_2\text{–AMP} + O_2 \longrightarrow \text{Luc} \cdot \text{L–Oxy}\star + \text{AMP} + CO_2 \quad \{1.2\}$$

$$\text{Luc} \cdot \text{L–Oxy}\star \longrightarrow \text{Luc} \cdot \text{L–Oxy} + h\nu \quad \{1.3\}$$

$$\text{Luc} \cdot LH_2\text{–AMP} + O_2 \longrightarrow \text{Luc} \cdot \text{L–AMP} + H_2O_2 \quad \{1.4\}$$

In an alternate pathway, LH_2-AMP is oxidized to form dehydroluciferin-AMP (L-AMP) and hydrogen peroxide, without any emission of light (Reaction 1.4) [89]. This is known as the dark reactions. The dark reactions account for approximately 20% of all luciferase activity [25]. Both of these products inhibit luciferase activity competitively against LH_2 [12]. It was found that the main cause for the quick decay of luminesence in firefly luciferase kinetics is accumulation of the inhibitors ([25]).

Table 1.1: The Body of FLCA Data (part 1)

Interpretation	Protein Pairs	System	
Quantitative†	9 interacting protein pairs	Plants	[41]
Quantitative	Peptides which interact upon radiation induced apoptosis	Mice	[42]
Qualitative	Membrane protein localization	Plants	[43]
Quantitative‡	NC complex formed when target RNA binds to RNA bound to NFLuc or CFLuc	*in vitro*	[44]
Qualitative	Histones H2A and H2B and *Arabidopsis* membrane proteins SYP61 and SYP51	Protoplasts	[45]
Quantitative	Amyloid β dimers/oligomers	*in vitro*	[46]
Qualitative	Large-scale screening of kinases and kinase inhibitors	*in vitro*	[47]
Qualitative	Fbox proteins known to interact and transcription factors	Filamentous ascomycetes	[48]
Qualitative	Proteins involved in forming integrin-link kinase-mediated protein complex	HEK	[49]
Qualitative	Andgrogen and liver receptor binding elements	*HeLa* human cells	[50]
Quantitative†	*Arabidopsis* FRB and human FKBP; 8 ARFs and 12 AUX proteins	Protoplasts	[51]
Qualitative	Kinase and regulator proteins	Plants	[52]
Qualitative	Bacterial pathogenic effector and potential tomato target proteins	Plants	[53]
Quantitative	Chemokines and receptor proteins	Human breast cancer cells	[54]
Qualitative	High-motility-group box protein and flu virous nucleoproteins	HEK	[55]
Qualitative	(review)	plant	[56]
Quantitative	Oncological kinases	(review)	[57]
Quantitative	Cellular defense proteins and their activators	HEK	[58]
Quantitative	Chimokene ligands	*homo sapiens* mammary cells	[59]
Qualitative	protein kinase and interaction partners during drought	Protoplasts	[60]

†: Papers which claim linear correlation between RLU and K_d. ‡: Papers which obtained saturation curves.

Table 1.2: The Body of FLCA Data (part 2)

Interpretation	Protein Pairs	System	
Quantitative	Drug and drug targets	(review)	[61]
Qualitative	Calcium sensor and activator proteins	Protoplasts	[62]
Qualitative	Rapamycin-dependent interactions between FRB and FKBP proteins	Plants	[63]
Qualitative	Receptor kinase and signaling proteins	Protoplasts and Plants	[64]
Quantitative	α syn nuclein oligomers	mice	[65]
Qualitative	Adipose hormone and potential ligands	Yeast	[66]
Quantitative	Apoptosome complex proteins	HEK	[67]
Quantitative	(review)	*in vivo*	[69]
Qualitative	Tumor necrosis factor protein and target proteins	HEK	[70]
Quantitative	Ubiquitin modifier and target proteins	Plants	[71]
Qualitative	(review)	*in vivo*	[72]
Quantitative	(review)	*in vivo*	[73]
Qualitative	CpG-site binding protein complex proteins	Leaves and protoplasts	[74]
Qualitative	Viral and glycolytic enzyme proteins	HEK	[75]
Qualitative	Chemokine receptor and target scaffolding proteins	Human breast cancer cells	[76]
Quantitative	Voltage gated channel complex proteins	HEK	[77]
Quantitative	(review)	Plants	[78]
Quantitative	Kinase activity which disrupts linker between enzyme domains	Human glioma cells	[79]
Qualitative	Anti-viral targets	(review)	[80]
Quantitative	Auxin uptake and efflux proteins	Plants	[81]
Qualitative	Protein complex that associates with the circadian clock	Protoplasts	[82]
Qualitative	Gibberellin signaling proteins	Plants	[83]
Quantitative	Deacetylase and its activator adn repressor proteins	HEK	[84]
Quantitative	RNA binding protein and repressor protein	Plants	[85]
Quantitative	Fungal transcription factor complex proteins	Fungi	[86]
Quantitative	Repressor and adapter protein targets	Protoplasts	[87]

Chapter 2
The Mathematical Model

2.1 Creation of the mathematical model

2.1.1 Existing models of firefly luciferase

Of interest to us, the kinetics of full length firefly luciferase and NFLuc have significant differences [3, 38]. Although currently mathematical models of full legnth firefly luciferase exist, certain key components are not taken into account in these models [17, 20]. In analyzing the kinetics of the FLCA, it is apparent that its kinetics are unique from both full length luciferase and NFLuc alone (Fig. 2.1, [38, 3]). The current models ignore many factors that have been previously shown experimentally to be significant. Therefore the conclusions of such full length models cannot explain the quantitative or qualitative nature of the FLCA. Hence, the first objective of this thesis became to incorporate these missing elements and understand how they cause the changes in kinetics.

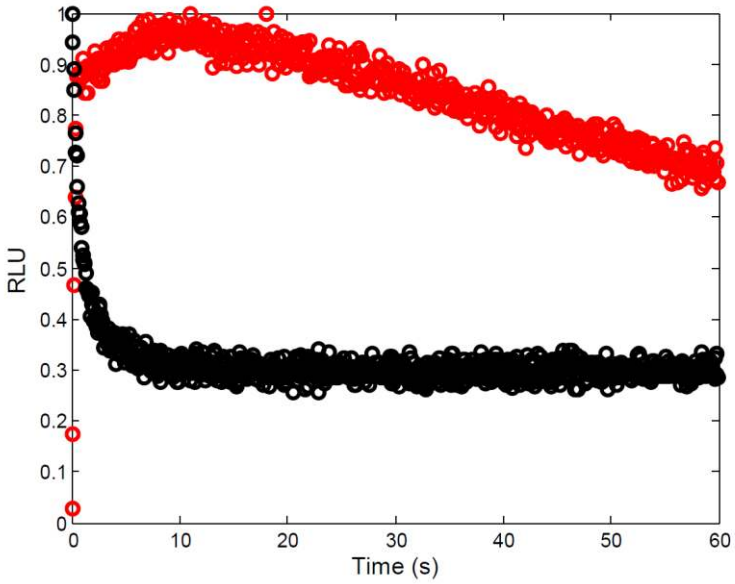

Figure 2.1: Luminescence kinetics of full length luciferase (black) and the FLCA (red) are different. Changes in the relative luminescence of full length luciferase and the FLCA *in vitro* were monitored every 0.2 s and 0.1 s, respectively, for 120 s in white 96-well plates. Differences in sampling time are due to the abilities of the luminometers used. Detected luminescence was normalized so that the maximum luminescence in each assay is 1. Notice that full length firefly luciferase kinetics has a sharp peak within 1 s followed by quick decay. On the other hand, split firefly luciferase has a more delayed peak and slower decay.

To date, three mathematical models exist which describe the firefly luciferase reaction pathway. The simplest model considers the system of reactions to be a simple Michaelis-Menten relationship of the form shown in equation 2.1 [17]. In this equation, k_{cat} is a constant of unit s^{-1}, expressing the production of luminescence by luciferase as a velocity.

$$\frac{dLight}{dt} = \frac{k_{cat} \cdot [enzyme] \cdot [substrate]}{K_m + [substrate]} \tag{2.1}$$

The most apparent problem with this assumption is that it only takes one substrate (LH_2) into account. ATP is a necessary substrate for the luciferase reaction, and it has a K_d of 160 μM, an order of magnitude higher than the K_d of LH_2 (16 μM) [6, 38]. In addition, the main cause of the quick decay of the firefly luciferase kinetics is product inhibition and this is not incorporated [25]. Another model incorporates this into a similar steady-state equation but with product inhibition incorporated (equation 2.2) [35]. In this equation, k_{cat} is a constant of unit s^{-1}, expressing the production of luminescence by luciferase as a velocity.

$$\frac{dLight}{dt} = \frac{[enzyme] \cdot k_{cat}}{1 + \frac{K_s}{[substrate]} + \frac{K_s \cdot [product]}{K_p \cdot [substrate]}} \tag{2.2}$$

Although this equation encompasses more of the reaction than the model described previously, the equation simplifies the random addition of two substrates, LH_2 and ATP, to the enzyme to a single substrate binding event. It fails to recognize the different affinities of the substrates and the two products, L-oxy and L-AMP. This is demonstrated by the model itself when it was found that curve fits produced very different substrate affinities and catalytic rates depending upon the concentration of substrate present [35].

A model constructed by Mannienen et al incorporates every binding and catalysis rate that luciferase undergoes [24]. However the adenylation step in this model is considered a one-way reaction. In addition, it does not account for dark reactions or the formation of L-AMP. The model also incorporated a regeneration step for the substrates, LH_2 and ATP, although this was not experimentally observed [24].

Model goals In summary, these existing models are not sufficient to understand the FLCA. The first objective of this thesis is to model the entire set of binding and catalysis events that luciferase performs. The complete conceptual understanding of the firefly luciferase reaction pathway includes the random addition of LH_2 and ATP, the reversible adenylation step, and either the production of excited L-oxy or L-AMP after oxidation. Luciferase is then reversibly inhibited by its products, which have different inhibition affinities (K_is). After completion of this conceptual model, it then should be adapted to represent the FLCA by incorporating NFLuc and the NC complex interactions.

2.1.2 The basis for the FLCA model

NFLuc has catalytic activity NFLuc alone can perform the adenylation and oxidation reactions, although the activity is 10^{-5} fold of the full length [38]. CFLuc forms the "active site" by coupling the adenylation and oxidation steps [32, 3]. The relative oxidation rate of the N domain alone is approximately 100 times less than full length luciferase [3]. Since

NFLuc and CFLuc are continuously binding and unbinding, depending upon the affinity of the protein pair attached, the activity of NFLuc alone during the FLCA will not necessarily be as minimal as that of NFLuc alone. Previous data suggests that the C domain of firefly luciferase undergoes a conformational change, allowed by the flexible linker region which connects it to the N domain. This conformational change allows for improved contact by the catalytic residues [3, 38]. Since CFLuc will continuously bind and unbind NFLuc during the FLCA, it is reasonable that it might have a significant effect upon the luminescent yield. The model will therefore incorporate a set of equations representing the binding and catalysis activities of NFLuc when not interacting with CFLuc (Fig. 2.2).

Effects of removing the C domain on the adenylation step Previous models of full length firefly luciferase have focused almost solely on the oxidation step of the reaction (Reaction 1.4), as this is the point when light is released. Only one model of the three existing models considered adenylation [24]. However, previous data suggests that the removal of the C domain has significant effects on the adenylation step [6, 8, 3, 38]. A series of mutagenesis experiments by Branchini et al mutated the two primary catalysis-enhancing residues on the C domain, Lys529 and Lys443 [6, 8]. The oxidation rate of the mutant decreases by 10^5 times compared to full length luciferase, while the adenylation rate drops 100 times [6]. In the same experiments, it was found that the affinity to both ATP and LH_2 substrates increased about 5 times [6]. Similar relative changes were found in a study comparing full length luciferase and NFLuc alone directly [38]. These studies were used as the primary sources for estimates concerning binding and catalysis rates by NFLuc and the NC complex in the model of the FLCA reactions.

2.1.3 The system of differential equations representing the FLCA

In order to understand the reasons for the different kinetics of the FLCA and their implications for data analysis, a mathematical model was created that describes the set of reactions of split firefly luciferase. The model was based on the conceptual model outlined above, and with the additional consideration of interacting and non-interacting NFLuc and CFLuc.

Model assumptions Our assumptions in the created model are summarized in (Fig. 2.2). Briefly, we assume that NFLuc and CFLuc reconstitute the "active site" upon the association of the protein pair fused to NFLuc and CFLuc [88]. ATP and LH_2, the substrates of firefly luciferase, can bind to NFLuc independently from CFLuc [7]. With both substrates bound, NFLuc catalyzes the adenylation and oxidation reactions but at a much lower rate than when CFLuc is present [1, 3]. The reconstituted "active site" is disrupted by constant dissociation of the protein pair fused to NFLuc and CFLuc. The two products, L-oxy and L-AMP, inhibit luciferase competitively and do not dissociate instantly upon formation [25, 12]. L-oxy is the light emitter and the primary product, while L-amp does not produce light (dark reaction)[25]. The frequency of the dark reactions increases when the enzyme is split [8]. A system of ordinary differential equations (ODEs) were written based on these assumptions (ODE 2.1.3) and initial estimates for the parameters were obtained from the literature (Table 2.1).

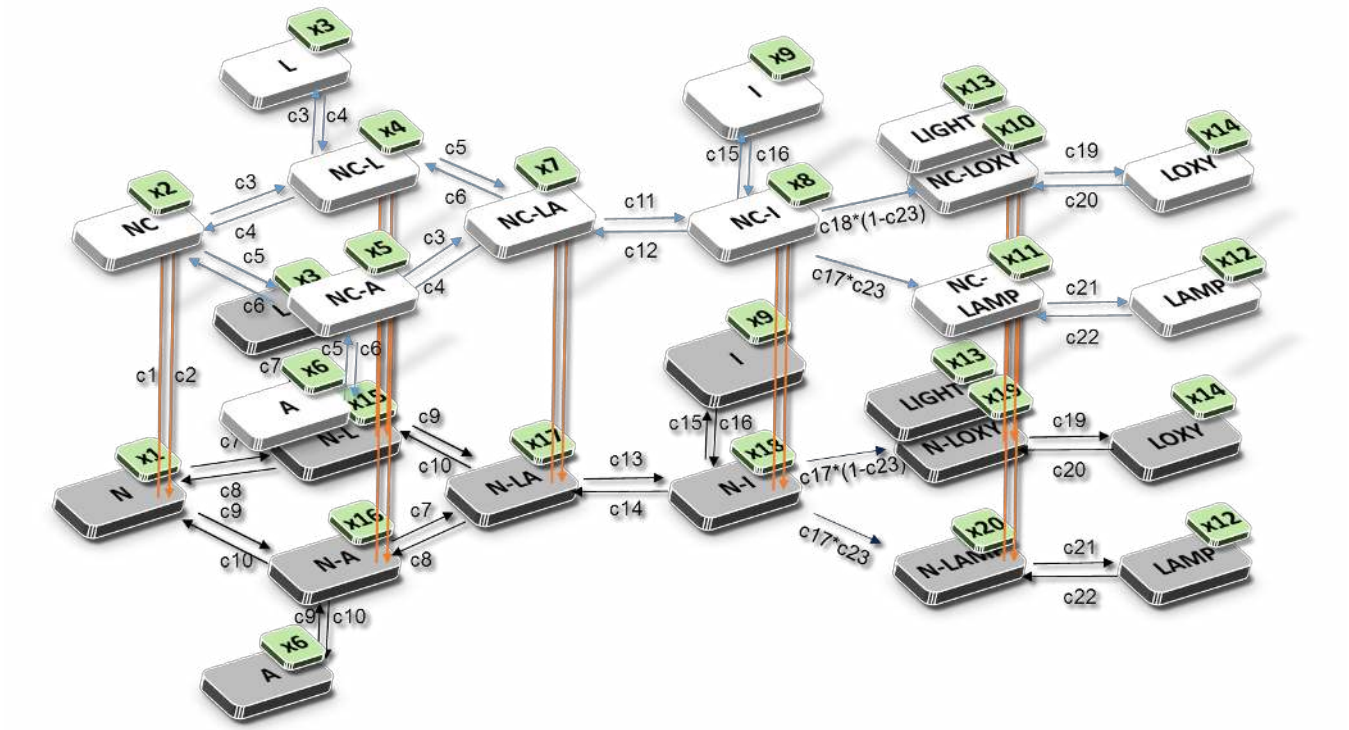

Figure 2.2: Diagram describing the complete set of interactions used to develop a mathematical model for the FLCA. The interaction of the protein pair (orange arrows) fused to NFLuc (grey panels) and CFLuc forms an NC complex (white panels) and reconstitutes enzymatic activity. The reconstituted activity produces luminescence by the adenylation and oxidation of LH_2. NFLuc contains all known substrate binding residues and can catalyze the reactions on its own, so we assume that some luminescence can be produced without the interaction of the protein pair [38, 3]. The mathematical model takes into account both NC complex interactions and the interactions of NFLuc only. The equations describing the reactions of NFLuc mirror that of the NC complex. "x" refers to variable number in the model, and "c" refers to the reaction rate parameter. Association rates are given odd numbered parameters, where applicable. N: NFLuc. NC: Interacting NFLuc and CFLuc. A: ATP. L: LH_2. NC-A: NC bound to ATP. NC-L: NC bound to LH_2. NC-LA: NC bound to both substrates. NC-I: NC bound to the intermediate, LH_2-AMP. I: Free LH_2-AMP. NC-LOXY: NC bound to L-oxyluciferin. NC-LAMP: NC bound to L-AMP. LOXY: Free L-oxyluciferin. LAMP: Free L-AMP. LIGHT: Observed luminescence. N-A: N domain bound to ATP. N-L: N bound to LH_2. N-LA: N bound to both substrates. N-I: N bound to the intermediate, LH_2-AMP. N-LOXY: N bound to oxyluciferin. N-LAMP: N bound to L-AMP. Not shown: CFLuc binding/unbinding (x_{21}).

ODE 2.1.3 (2.3)

System of ordinary differential equations describing the FLCA

$$\frac{dx_1}{dt} = -c_1 \cdot x_1 \cdot x_{21} + c_2 \cdot x_2 - c_9 \cdot x_1 \cdot x_6 + c_{10} \cdot x_{16} - c_7 \cdot x_1 \cdot x_3 + c_8 \cdot x_{15} - c_{24} \cdot x_1 \cdot x_{14} + c_{25} \cdot x_{19} - c_{26} \cdot x_1 \cdot x_{12} + c_{27} \cdot x_{20} - c_{15} \cdot x_1 \cdot x_9 + c_{16} \cdot x_{18} \tag{2.4}$$

$$\frac{dx_2}{dt} = c_1 \cdot x_1 \cdot x_{21} - c_2 \cdot x_2 - c_3 \cdot x_2 \cdot x_3 + c_4 \cdot x_4 - c_5 \cdot x_2 \cdot x_6 + c_6 \cdot x_5 - c_{21} \cdot x_2 \cdot x_{12} + c_{22} \cdot x_{11} - c_{19} \cdot x_2 \cdot x_{14} + c_{20} \cdot x_{10} - c_{15} \cdot x_2 \cdot x_9 + c_{16} \cdot x_8 \tag{2.5}$$

$$\frac{dx_3}{dt} = -c_3 \cdot x_2 \cdot x_3 + c_4 \cdot x_4 - c_3 \cdot x_5 \cdot x_3 + c_4 \cdot x_7 - c_7 \cdot x_1 \cdot x_3 + c_8 \cdot x_{15} - c_7 \cdot x_{16} \cdot x_3 + c_8 \cdot x_{17} \tag{2.6}$$

$$\frac{dx_4}{dt} = c_3 \cdot x_2 \cdot x_3 - c_4 \cdot x_4 - c_5 \cdot x_4 \cdot x_6 + c_6 \cdot x_7 + c_1 \cdot x_{15} \cdot x_{21} - c_2 \cdot x_4 \tag{2.7}$$

$$\frac{dx_5}{dt} = -c_3 \cdot x_5 \cdot x_3 + c_4 \cdot x_7 + c_5 \cdot x_2 \cdot x_6 - c_6 \cdot x_5 + c_1 \cdot x_{16} \cdot x_{21} - c_2 \cdot x_5 \tag{2.8}$$

$$\frac{dx_6}{dt} = -c_5 \cdot x_2 \cdot x_6 + c_6 \cdot x_5 - c_5 \cdot x_4 \cdot x_6 + c_6 \cdot x_7 - c_9 \cdot x_1 \cdot x_6 + c_{10} \cdot x_{16} - c_9 \cdot x_{15} \cdot x_6 + c_{10} \cdot x_{17} \tag{2.9}$$

$$\frac{dx_7}{dt} = c_3 \cdot x_5 \cdot x_3 - c_4 \cdot x_7 + c_5 \cdot x_4 \cdot x_6 - c_6 \cdot x_7 + c_1 \cdot x_{17} \cdot x_{21} - c_2 \cdot x_7 - c_{11} \cdot x_7 + c_{12} \cdot x_8 \tag{2.10}$$

$$\frac{dx_8}{dt} = c_{11} \cdot x_7 - c_{12} \cdot x_8 + c_1 \cdot x_{18} \cdot x_{21} - c_2 \cdot x_8 - c_{18} \cdot x_8 + c_{15} \cdot x_2 \cdot x_9 - c_{16} \cdot x_8 \tag{2.11}$$

$$\frac{dx_9}{dt} = -c_{15} \cdot x_2 \cdot x_9 + c_{16} \cdot x_8 - c_{15} \cdot x_1 \cdot x_9 + c_{16} \cdot x_{18} \tag{2.12}$$

$$\frac{dx_{10}}{dt} = c_{18} \cdot x_8 \cdot (1 - c_{23}) + c_1 \cdot x_{19} \cdot x_{21} - c_2 \cdot x_{10} + c_{19} \cdot x_2 \cdot x_{14} - c_{20} \cdot x_{10} \tag{2.13}$$

$$\frac{dx_{11}}{dt} = c_{18} \cdot c_{23} \cdot x_8 + c_1 \cdot x_{20} \cdot x_{21} - c_2 \cdot x_{11} + c_{21} \cdot x_2 \cdot x_{12} - c_{22} \cdot x_{11} \tag{2.14}$$

$$\frac{dx_{12}}{dt} = -c_{21} \cdot x_2 \cdot x_{12} + c_{22} \cdot x_{11} - c_{26} \cdot x_1 \cdot x_{12} + c_{27} \cdot x_{20} \tag{2.15}$$

$$\frac{dx_{13}}{dt} = c_{18} \cdot x_8 \cdot (1 - c_{23}) - x_{13} + c_{17} \cdot x_{18} \cdot (1 - c_{23}) \tag{2.16}$$

$$\frac{dx_{14}}{dt} = -c_{19} \cdot x_2 \cdot x_{14} + c_{20} \cdot x_{10} - c_{24} \cdot x_1 \cdot x_{14} + c_{25} \cdot x_{19} \tag{2.17}$$

$$\frac{dx_{15}}{dt} = c_7 \cdot x_1 \cdot x_3 - c_8 \cdot x_{15} - c_9 \cdot x_{15} \cdot x_6 + c_{10} \cdot x_{17} - c_1 \cdot x_{15} \cdot x_{21} + c_2 \cdot x_4 \tag{2.18}$$

$$\frac{dx_{16}}{dt} = c_9 \cdot x_1 \cdot x_6 - c_{10} \cdot x_{16} - c_7 \cdot x_{16} \cdot x_3 + c_8 \cdot x_{17} - c_1 \cdot x_{16} \cdot x_{21} + c_2 \cdot x_5 \tag{2.19}$$

$$\begin{aligned}\frac{dx_{17}}{dt} = &-c_{13} \cdot x_{17} + c_{14} \cdot x_{18} + c_9 \cdot x_{15} \cdot x_6 - c_{10} \cdot x_{17} + c_7 \cdot x_{16} \cdot x_3 \\ &- c_8 \cdot x_{17} - c_1 \cdot x_{17} \cdot x_{21} + c_2 \cdot x_7\end{aligned} \tag{2.20}$$

$$\begin{aligned}\frac{dx_{18}}{dt} = &c_{13} \cdot x_{17} - c_{14} \cdot x_{18} - c_1 \cdot x_{18} \cdot x_{21} + c_2 \cdot x_8 - c_{17} \cdot x_{18} + c_{15} \cdot x_1 \cdot x_9 \\ &- c_{16} \cdot x_{18}\end{aligned} \tag{2.21}$$

$$\frac{dx_{19}}{dt} = c_{17} \cdot (1 - c_{23}) \cdot x_{18} - c_1 \cdot x_{19} \cdot x_{21} + c_2 \cdot x_{10} + c_{24} \cdot x_1 \cdot x_{14} - c_{25} \cdot x_{19} \tag{2.22}$$

$$\frac{dx_{20}}{dt} = c_{17} \cdot c_{23} \cdot x_{18} - c_1 \cdot x_{20} \cdot x_{21} + c_2 \cdot x_{11} + c_{26} \cdot x_1 \cdot x_{12} - c_{27} \cdot x_{20} \tag{2.23}$$

$$\begin{aligned}\frac{dx_{21}}{dt} = &-c_1 \cdot x_{21} \cdot x_1 - c_1 \cdot x_{21} \cdot x_{15} - c_1 \cdot x_{21} \cdot x_{16} - c_1 \cdot x_{21} \cdot x_{17} \\ &- c_1 \cdot x_{21} \cdot x_{20} - c_1 \cdot x_{21} \cdot x_{19} + c_2 \cdot x_2 + c_2 \cdot x_4 + c_2 \cdot x_5 + c_2 \cdot x_{11} \\ &+ c_2 \cdot x_{10} \quad + c_2 \cdot x_7 - c_1 \cdot x_{21} \cdot x_{18} + c_2 \cdot x_8\end{aligned} \tag{2.24}$$

Applicability of ODEs to biological systems Ordinary differential equations express the change in a function with respect to a variable. In our case, some of the variables we consider are enzyme concentration and substrate concentration. When an equation is differentiated, the solution can be thought of as the rate of change, or slope of the function with respect to a variable. Since the rate of change is already known by previous experiments detailing the interaction pathways of enzymes, we can write the differential equations directly. As the changes in a biological system are occurring over time, these equations are written with respect to the change in time.

Differential equations are useful as many biological processes can be considered in terms of rates. The rate at which an enzyme binds its substrate, for example, can be expressed as k_{on}. This k_{on} can be directly and objectively measured, but when considering the amount of substrate bound at a given point in time, the rate can be modified to reflect the changing conditions, following the law of mass action. For example, the amount of substrate available to bind the enzyme will affect the amount of enzyme-substrate complex formed in the next time unit, although the k_{on} does not change. The amount of enzyme available will also affect this value.

Brief overview of the ODEs The variable and parameter assignments can be seen in Fig. 2.2. Association interactions are expressed by the appropriate forward parameter k_{on}.

We can then modify the association by the concentration of the two interacting species. For example, in equation 2.5, the interaction of NFLuc to ATP is expressed by the k_{on} parameter specific to this interaction, c_7, multiplied by the concentrations of NFLuc and ATP at time t. Reverse interactions are expressed by reverse rate parameters, k_{off}, which are also specific to that species. The dissociation of NFLuc-ATP complex is expressed by the k_{off} modified by the concentration of NFLuc-ATP at time t. The concentration of any given species is updated at every time unit by the appropriate rate. The concentration of NFLuc decreases at the rate k_{on}·NFLuc·ATP but increases at the rate k_{off}· NFLuc-ATP. The concentration of NFLuc, for example, is also affected by all of its other interaction and catalysis rates.

All reactions accrue by mathematical rules. For example in equation 2.13, the amount of L-oxy produced by the NC complex is modified by the rate 1-c_{23}. Parameter c_{23} represents the frequency of oxidation events which are dark reactions as a number between 0 and 1. In equation 2.16, which calculates the amount of light at time t, the concentration of light was corrected by subtraction of x_{13} at every time t. This is because light is not a cumulative property, but decays very quickly. The luminometers read and plot light at some set sampling point, which is equivalent to the model's incremental sampling point. This gives the effect of tracking the light produced at time t only, which is representative of experimental data collection, which usually occurs every 0.1 s.

Incorporation of protein-protein interactions The mathematical model (ODE 2.1.3) is applied to a protein pair to reflect experimental FLCA conditions. For this protein pair we chose the interacting pair p53 and mdm2. P53 is a tumor suppressor protein and mdm2 regulates it by binding to it [31]. The transactivation domain of p53 is bound by mdm2 with an affinity of 212 nM [31]. The transactivation domain of p53 (residues 15-29) was genetically attached to NFLuc, and whole mdm2 was similarly attached to CFLuc [28]. The transactivation domain of p53 binds mdm2 with a K_d of 212 nM, and their association and dissociation rates have been experimentally determined [31]. The relationship between the K_d and the association and dissociation rates is shown in equation 2.25.

$$K_d = \frac{k_{off}}{k_{on}} \tag{2.25}$$

The interaction between NFLuc and CFLuc is described by an association rate (c_1) and a dissociation rate (c_2). These rates are assumed to be the same as the association and dissociation rate of the protein pair themselves. *In vivo*, mdm2 causes the inactivation and degradation of p53 [31].

Table 2.1: Parameters Derived from the Literature.

Full length parameters		
Luciferin Affinity	7.2-15 μM	[38, 6]
ATP Affinity	160-230 μM	[38, 6]
Intermediate Affinity	4.7 μM	[6]
Net Adenylation Rate	0.001 s^{-1}	Estimated‡ [6]
Catalytic Activity	0.23 s^{-1}	[6]
NFLuc only parameters		
Luciferin Affinity	26-67 μM	[38, 6]
ATP Affinity	560-6900 μM	[38, 6]
Intermediate Affinity	0.55 μM	[6]
Net Adenylation Rate	0.00001 s^{-1}	Estimated‡ [6]
Catalytic Activity	0.0000311 s^{-1}	[6]
Shared parameters		
L-AMP Affinity	3.8 nM	[34, 25, 12]
Oxyluciferin Affinity	500 nM	[25, 12]
Dark Reaction Frequency	> 0.2	[25, 8]
Degradation of Split Luciferase	0.00136 s^{-1}	Calculated† [28]
Protein parameters		
P53/MDM2 Affinity	212 nM	[31]
k_{on} of P53 and MDM2	2 s^{-1}	[31]
k_{off} of P53 and MDM2	0.009 $nM^{-1}s^{-1}$	[31]
Nutlin-3/MDM2 Affinity	216-250 nM	Calculated†

Initial estimates for parameter values were taken from the literature where available. Some values were calculated from experimental results (†) or estimated (‡) from relative rate comparisons.

Chapter 3
Results and Discussion

3.1 The FLCA model agrees with experimental data

Previous independent studies suggest that kinetics of luminescence production in full length luciferase and the FLCA are different [3, 38, 21]. We conducted experiments which directly compare the kinetics of luminesence production in the FLCA and full length luciferase (Fig. 2.1). In this experiment, we used 50 nM each of p53-NFLuc and mdm2-CFLuc [28]. The protein pair p53 and mdm2 is known to interact with each other *in vitro* with a dissociation constant (K_d) of 212 nM [31]. NFLuc and CFLuc were fused to p53 and mdm2 as described previously [28].

In our experimental conditions, the luminescence kinetics of 150 nM full length firefly luciferase was measured after adding 75 μM LH_2 and 100 mM ATP. Full length firefly luciferase shows a sharp peak within the first second, followed by fast signal decay (Fig. 2.1). These kinetics are observed regardless of the different concentrations used (Fig. 3.1) [25]. The luminescence kinetics of split firefly luciferase shows a slower peak with slower signal decay (Fig. 2.1). Previous data shows that the kinetics of the peak of the FLCA kinetics are independent from protein concentrations used in the assays for protein pairs [28]. This result confirmed the previous suggestion that the kinetics of luminescence production in full length and split firefly luciferase are different. This result also suggested that the different luminescence kinetics are not due to insufficient substrate concentrations, or sensor artifacting, but rather other factors.

3.1.1 Estimation of NFLuc binding and catalysis rates

The adenylation rate was estimated by curve fitting to previously published NFLuc kinetic data [3]. We used the portion of the mathematical model which describes the binding and catalysis of NFLuc alone by removing the portions of the equations involving CFLuc (ODE 4.1.2). To curve fit the model to the previously published data, we digitized the data using PlotDigitizer (Fig. 3.2) [3]. Matlab's lsqcurvefit function was used to perform the curve fit. The literature provided initial estimates for parameters (Table 2.1). The curve fit produced initial estimates for the previously unknown forward and reverse NFLuc adenylation rates, as well as more optimized values for the interaction and catalytic rates of NFLuc alone (Table 3.2).

3.1.2 Estimation of NC complex binding and catalysis rates

Calculation of initial conditions The FLCA data used to estimate parameters was collected after incubation of p53-NFLuc and mdm2-CFLuc at 37℃ for 120 s. Therefore, prior to simulating the FLCA the initial concentration of NFLuc, CFLuc, and the NC complex was calculated.

It was shown previously that NFLuc and CFLuc degrades when incubated at 37 ℃ [28]. The activity of the FLCA at different lengths of incubation time was recorded previously

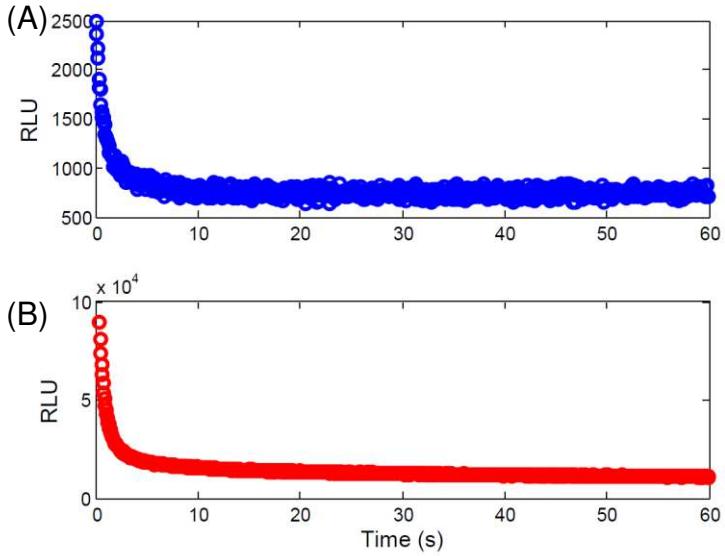

Figure 3.1: Kinetics of full length firefly luciferase is independent of concentration. (A) Kinetics at 150 nM of firefly luciferase. (B) Kinetics at 450 nM of firefly luciferase.

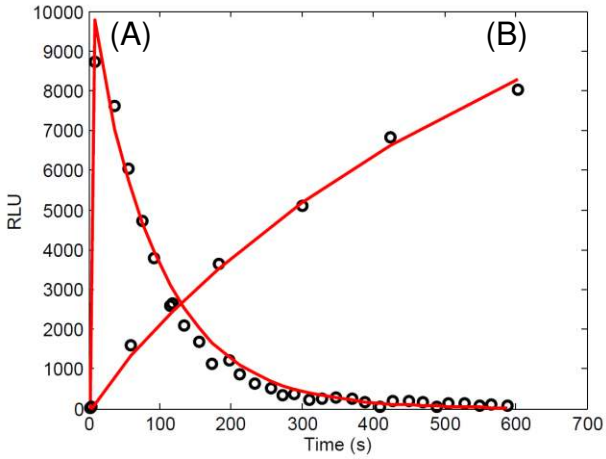

Figure 3.2: Parameter estimation using NFLuc alone *in vitro* luminescence kinetics data. Data originally published in [38] was digitized using Plot Digitizer [16]. Digitized data was curve fit to estimate parameters unavailable from previously published papers. (A) The addition of 3.7 nM LH_2-AMP to 1 μM NFLuc shows a sharp peak. This curve fit provided an estimation of the adenylation forward and reverse rates. (B) When a substrate solution (300 μM LH_2, 10 mM ATP) is added to 1 μM NFLuc, the luminescence kinetics have a slow rise and no peak. This curve fit provided more optimized values for the available NFLuc only binding and catalysis rates.

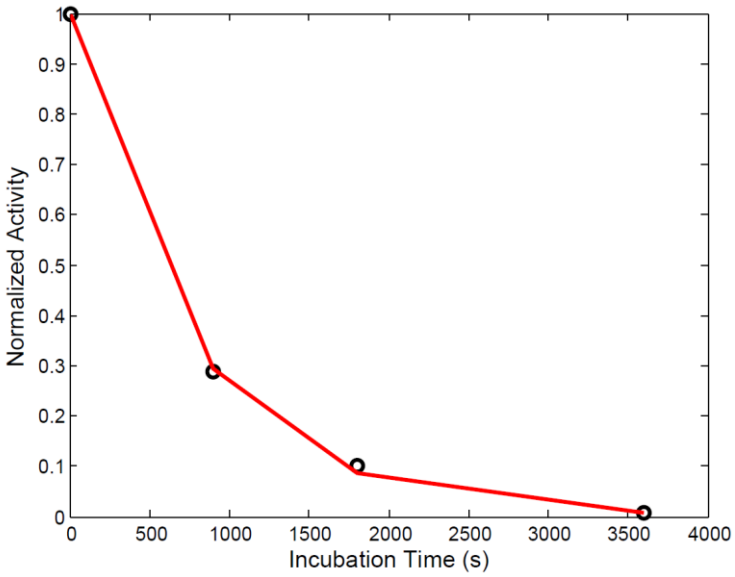

Figure 3.3: Determination of the degradation rate of NFLuc and CFLuc at 37 ℃. Previously the heat stability of NFLuc and CFLuc was analyzed by measuring the activity after incubation times ranging from 0 to 60 minutes at 37 ℃. To calculate the degradation rate, the RLU values were digitized using PlotDigitizer and the maximum RLU values were extracted. The RLU value for no incubation time was considered 100% activity. This was curve fit to an equation describing degradation (Eqn. 3.1). The degradation rate was found to be 0.00136 s^{-1}.

and used in this calculation. The maximum luminesence values for each incubation time were normalized to 100% or less activity and curve fit to equation 3.1 (Fig. 3.3) [28]. The degradation rate of NFLuc and CFLuc at 37 ℃ was calculated to be 0.00136 s^{-1}.

$$Activity = e^{-DegradationRate*Time} \tag{3.1}$$

After obtaining an estimate for the degradation rate at 37℃, a system of equations was written to describe the interaction of two proteins at the rates k_{on} and k_{off}, and their degradation at 0.00136 s^{-1} (See appendix C). The amount of NFLuc, CFLuc, and NC complex at 120 s were used as the initial concentrations upon the addition of substrates (Fig. 3.4(A)).

Estimation of NC complex binding and catalysis rates We used the parameter estimates from the literature and the improved estimates from the curve fit to NFLuc only data (Fig. 3.2) as initial estimates for NC complex parameters. We curve fit the mathematical model describing the *in vitro* FLCA to experimental data obtained with the protein pair NFLuc-p53 and CFLuc-mdm2. The predicted luminescence after optimization of the NC complex parameters closely matches the experimental data, as shown in Fig. 3.5.

We also looked at the ability of the model to fit other data sets with different concentrations of NFLuc-p53 and CFLuc-mdm2 (Fig. 3.6). These experiments were performed under

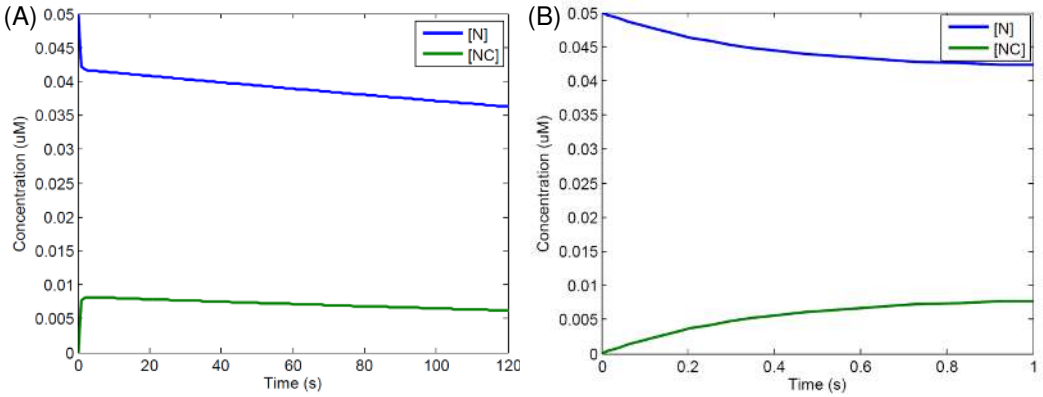

Figure 3.4: Determination of the initial concentration of NC complex *in silico*. Initial concentration of free NFLuc-p53, free CFLuc-mdm2, and NC complex was modeled using the affinity for p53 and mdm2 from the literature [31]. (A) For luminescence kinetic data with incubation at 37 ℃(shown in Fig. 2.1, Fig. 3.5), the degradation rate was included in the calculation of initial conditions. (B) For luminescence kinetics data without any incubation (see Fig. 3.6), probes were not incubated, but an average experimental delay of approximately 1 s is assumed due to the use of 96-well plates.

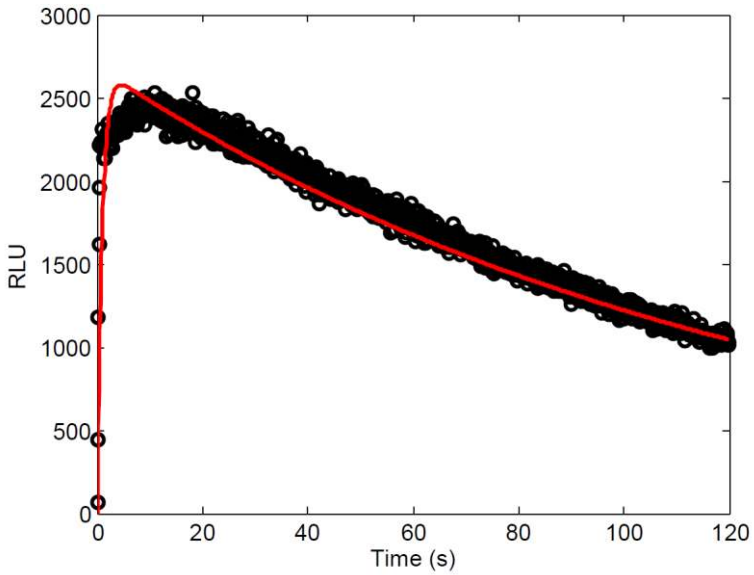

Figure 3.5: Model simulation (red) of the luminesence kinetics of NFLuc-p53 and CFLuc-mdm2 using *in vitro* FLCA compared to the data (black) after optimization. The values for the parameters in the mathematical model were estimated in three steps. Parameter values were taken from the literature when able, or calculated from previous data (Table 1.1). Additional parameter values were estimated by curve fitting the model to the luminescence kinetics of NFLuc only [38] (Fig. 3.2). Finally, NC complex binding and catalysis rates were optimized by curve fitting (red) to the luminescence kinetics of NFLuc-p53 and CFLuc-mdm2 using FLCA (black).

the same conditions as Fig. 3.5, but there was no incubation step. However, it is reasonable to expect some delay after addition of the enzyme solution to the 96-well plate and the injection of the substrate solution. To reflect this, the 'incubation' time was estimated to be 1 s. The amount of NFLuc, CFLuc, and NC complex at 1 s were used as the initial concentrations upon the addition of the substrates. No parameters were optimized for these data sets with the exception of the photomultiplier tube's effect upon the measured RLU. The photomultiplier tube automatically magnifies the signal it detects upon detecting a photon, either by a user-defined value or by an internal calculation.

The model reasonably fits the data with the exception of early time points. For these experiments, 50 μL of solution containing p53-NFLuc and mdm2-CFLuc are first added to a well in a 96-well plate. Then the luminometer injects a 50 μL substrate solution directly into the well, and measures the luminescence immediately after. The model's equations assume a homogenous mixture of all species, such that it is equally likely for any compound to come into contact with another compound. For the very early time points of the FLCA, however, this may not be true.

3.1.3 The mathematical model predicts that the interaction of NFLuc and CFLuc reconstitutes full length activity

The results of the curve fitting brought us a quantitative understanding of the luminescence production in FLCA. A direct comparison of the experimental and estimated values are shown in Table 3.1, and the raw rate parameters are shown in Table 3.2. First, when the "active site" is reconstituted through the protein interaction of p53 and mdm2, the affinity of LH_2 to NFLuc increases from 27.5 μM to 16 μM. This is comparable to the full length affinity to LH_2, which has been measured between 7.2-16 μM [6, 38]. The affinity of ATP increases from 683 μM to NFLuc alone to 160 μM to the NC complex. This is also within the range of previously obtained full length affinity to ATP (160-230 μM) [6, 38]. The k_{on} and k_{off} values can be seen in Table 3.2.

The net adenylation rate of the NC complex was estimated to be 500 s^{-1}, which is about 10^5 times higher than the value we obtained for NFLuc alone (0.004 s^{-1}). Previous data suggests that full length luciferase would have a 100 times higher adenylation rate than that in a full length mutant in which the C domain's catalytic residues were selectively mutated [6]. We believe that NFLuc alone has a much lower adenylation rate than that in the mutant luciferase. The oxidation rate of the NC complex, 0.219 s^{-1}, is very close to experimental values for full length luciferase (0.23 s^{-1}) [6]. The oxidation rate of NFLuc ($4{\cdot}10^{-7}s^{-1}$) is lower than the experimental values for a full length mutant in which the C domain's catalytic residues were selectively mutated ($3.11 \cdot 10^{-5}s^{-1}$) [6].

The frequency of dark reactions was previously predicted to increase from the 20% of full length luciferase, and the curve fitting results suggest that both the NC complex and NFLuc alone have a 29% dark reaction frequency [8]. The affinity of the intermediate to the NC complex and NFLuc alone were both estimated to be 45 nM. This value is much lower than previous experimental values for full length luciferase (4.7 μM) and a full length mutant in which the C domain's catalytic residues were selectively mutated (550 nM)

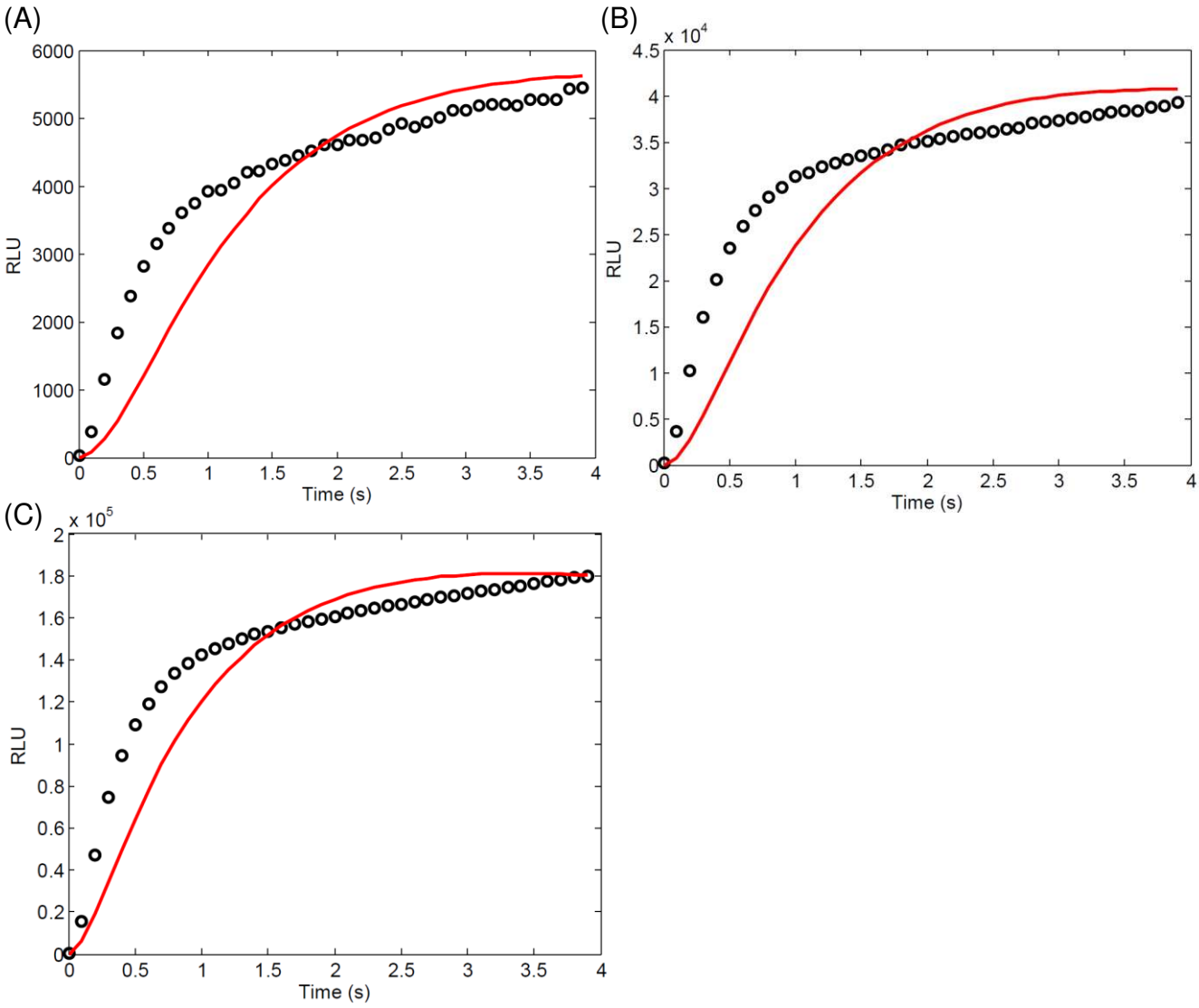

Figure 3.6: The mathematical model (red) reasonably matches data (black) at varying concentrations of NFLuc-p53 and CFLuc-mdm2. (A) 50 nM of NFLuc-p53 and CFLuc-mdm2 each. (B) 150 nM of NFLuc-p53 and CFLuc-mdm2 each. (C) 450 nM of NFLuc-p53 and CFLuc-mdm2 each. Each simulation was separately optimized with respect to the effects of the detection lens (photomultiplier tube). Data obtained from [28].

Table 3.1: Comparison of Experimental and Estimated Values.

Parameter	Full length †	NC complex ‡	NFLuc ‡	NFLuc †
LH_2 Affinity	7.2-15 μM	16 μM	27.5 μM	26-67 μM
ATP Affinity	160-230 μM	160 μM	683 μM	560-6900 μM
LH_2-AMP Affinity	4.7 μM	45 nM	45 nM	550 nM
L-oxy Affinity	500 nM	70 nM	70 nM	–
L-AMP Affinity	3.8 nM	460 pM	23 pM	–
Net Adenylation Rate	100 §	500 s^{-1}	.004 s^{-1}	1 §
Oxidation Rate	0.23 s^{-1}	0.219 s^{-1}	$4{\cdot}10^{-7}s^{-1}$	$3.11\ {\cdot}10^{-5}s^{-1}$
Dark Reaction Frequency	0.2	0.29	0.29	> 0.2

†: Values obtained from the literature [6, 38]. Values for luciferase without the catalytic residues on the C domain are also reported here. ‡: Estimated values obtained from the curve fit. § : Values are relative to each other (e.g., a full length mutant in which the C domain's catalytic residues were selectively mutated has 100 times slower adenylation than the wild type.) [6].

[6]. However these experimental values suggest that the intermediate has higher affinity to the mutant than to the wild type luciferase. Therefore our estimation, although quite low, is tangentially supported by previous data. We believe that NFLuc, both alone and in the NC complex, has a much higher affinity to the intermediate than the mutant luciferase.

The estimated values for the affinity of the inhibitors is also very low. The affinity of L-amp to the NC complex and NFLuc alone is 460 pM, about 10 times higher than the experimental value of 3.8 nM for full length luciferase [12, 25]. The affinity of L-oxy to the NC complex and NFLuc alone is 70 nM, about 10 times higher than the previous experimental value of 500 nM for full length luciferase [12, 25]. Since full length mutant was observed to have 10 times lower affinity to the intermediate, it seems reasonable that the mutant might also have 10 times lower affinity to the products as they are structurally similar [6]. We therefore believe that NFLuc, both alone and in the NC complex, has much lower affinity to the intermediate and the products than the full length mutant or wild type luciferase.

3.1.4 The mathematical model reproduces the IC-50 curve of nutlin-3

The IC-50 can be defined as the point at which the observed binding of two proteins is decreased by 50% by the ligand in question [91]. Ohmuro et al previously examined the IC-50 of nutlin-3 using the *in vitro* FLCA [28]. Nutlin-3 inhibits the p53-mdm2 interaction by binding to mdm2. The K_i of nutlin-3 was estimated using equation 3.2 [90]. The K_i is an objective measurement of the affinity of a protein and its inhibitor [90]. The IC-50 and the K_i are not perfectly correlated since the inhibitory ligand must compete with the target protein's other binding partner, among other factors [90]. A correction factor which takes into account the strength of binding between the target protein and its binding partner and the concentration of the proteins is therefore applied to the observed IC-50. Since the IC-50 is 350 ± 25 nM with 100 nM of p53-NFLuc and mdm2-CFLuc, the calculated K_i is 216-250

Table 3.2: Parameters Values from the Curve Fit

c_1	$K_{d,f}$ Association of P53 and MDM_2	$9.2{\cdot}10^6\ M^{-1}s^{-1}$
c_2	$K_{d,r}$ Dissociation of P53 and MDM_2	$2\ s^{-1}$
c_3	ka_f Association of LH_2 to NC Complex	$1.84{\cdot}10^8\ M^{-1}s^{-1}$
c_4	ka_r Dissociation of LH_2 from NC Complex	$3{\cdot}10^3\ s^{-1}$
c_5	kl_f Association of ATP to NC Complex	$3{\cdot}10^7\ M^{-1}s^{-1}$
c_6	kl_r Dissociation of ATP from NC Complex	$4.8{\cdot}10^3\ s^{-1}$
c_7	kl_{f2} Association of LH_2 to NFLuc	$1.84{\cdot}10^8 M^{-1}s^{-1}$
c_8	kl_{r2} Dissociation of LH_2 from NFLuc	$5.05{\cdot}10^3\ s^{-1}$
c_9	ka_{f2} Association of ATP to NFLuc	$3{\cdot}10^7\ M^{-1}s^{-1}$
c_{10}	ka_{r2} Dissociation of ATP from NFLuc	$2.05{\cdot}10^4\ s^{-1}$
c_{11}	kIf Adenylation rate, forward, NC complex	$5.01{\cdot}10^2 s^{-1}$
c_{12}	kIf Adenylation rate, reverse, NC complex	$1.08{\cdot}10^{-2}s^{-1}$
c_{13}	ki_f Adenylation rate, forward, NFLuc	$5{\cdot}10^{-2}s^{-1}$
c_{14}	ki_r Adenylation rate, reverse, NFLuc	$1.1{\cdot}10^{-2}s^{-1}$
c_{15}	kIf Association of Intermediate	$7.77{\cdot}10^7\ M^{-1}s^{-1}$
c_{16}	kIf Dissociation of Intermediate	$3.47\ s^{-1}$
c_{17}	$kcat$ Catalytic Rate NFLuc	$4{\cdot}10^{-7}s^{-1}$
c_{18}	$kcat$ Catalytic Rate NC complex	$2.19\dot{1}0^{-1}s^{-1}$
c_{19}	ki_f Association of Oxyluciferin to NC Complex	$8.3{\cdot}10^6 M^{-1}s^{-1}$
c_{20}	ki_r Dissociation of Oxyluciferin from NC Complex	$6.13{\cdot}10^{-1}s^{-1}$
c_{21}	ki_{f2} Association of L-AMP to NC Complex	$5{\cdot}10^7 M^{-1}s^{-1}$
c_{22}	ki_{r2} Dissociation of L-AMP from NC Complex	$2.3{\cdot}10^{-5}s^{-1}$
c_{23}	Dark Reaction Frequency	$2.87\dot{1}0^{-1}$
c_{24}	ki_f Association of Oxyluciferin to NFLuc	$8.3{\cdot}10^6 M^{-1}s^{-1}$
c_{25}	ki_r Dissociation of Oxyluciferin from NFLuc	$6.13{\cdot}10^{-1}s^{-1}$
c_{26}	ki_{f2} Association of L-AMP to NFLuc	$5{\cdot}10^7 M^{-1}s^{-1}$
c_{27}	ki_{r2} Dissociation of L-AMP from NFLuc	$2.3{\cdot}10^{-5}s^{-1}$
c_{28}	Heat Degradation	$1{\cdot}10^{-3}\ s^{-1}$

Parameter values after optimization by curve fitting mathematical model to kinetic data. Protein pair used in obtaining the experimental data for the curve fit was p53 and mdm2.

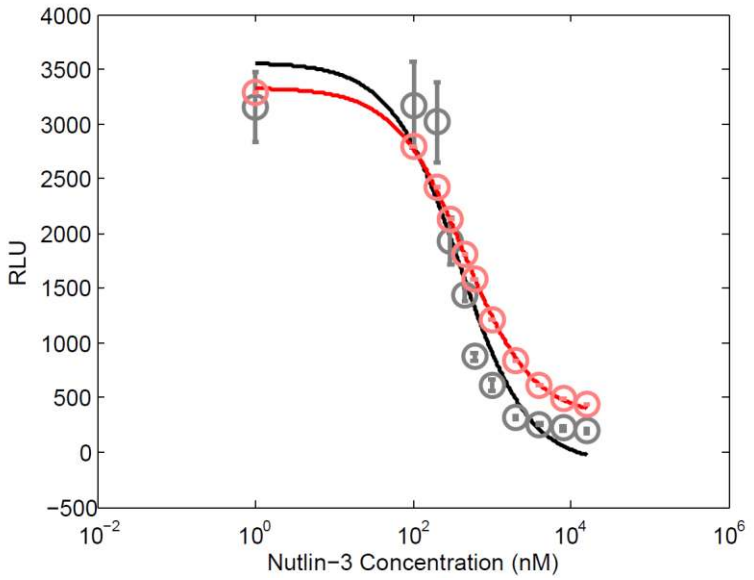

Figure 3.7: Predicted nutlin-3 IC-50 curve (red) using *in vitro* FLCA agrees with the data (black). Experimental RLU values from [28] at 0.2 s (black) compared with model predicted RLU values (red) across a range of nutlin-3 concentrations, a specific binding inhibitor of mdm2. The calculated IC-50 of the experimental data is 390 nM, while the simulation IC-50 is 440 nM.

nM [28]. The k_{on} was estimated at $1 \cdot 10^{-7} M^{-1} s^{-1}$ [29], and the initial guess for the K_i was 235 nM.

$$K_i = \frac{IC_{50}}{\frac{[NFLuc]}{K_d} + 1} \tag{3.2}$$

The mathematical model was modified to reflect the three way interaction by the addition of ODEs describing the interaction of an inhibitor to a protein fused to CFLuc (See appendix C) to ODE 2.1.3. The data used to calculate the IC-50 in the previously published study were luminescence values (RLU) sampled at 0.2 s over a range of nutlin-3 concentrations. A total of 10 different concentrations of nutlin-3 were used, from 1 nM to 16 μM [28]. The initial conditions of p53 and mdm2 were calculated to be incubated to equilibrium prior to the addition of nutlin-3, as described in [28]. The model was then used to simulate the IC-50 experiment, and equation 3.3 was used to calculate the IC-50 using the resulting data points [91]. The IC-50 value calculated by nonlinear regression to this equation gave 390 nM for the experimental data and 440 nM for the model (Fig. 3.7).

$$Activity = max + \frac{(min - max)}{(1 + (\frac{[nutlin-3]}{IC-50}))} \tag{3.3}$$

Conclusion These results show that the model accurately represents the FLCA system. The model is capable of matching NFLuc alone kinetics, experimental data over the long or short term, several concentrations of NFLuc and CFLuc, and the nutlin-3 IC-50 curve. The estimated values for the binding and catalysis rates are not unreasonable when compared with values from the literature. We believe this demonstrates the model is representative of the FLCA, and now we will use the model to analyze the FLCA data as being qualitative or quantitative in nature.

3.2 Predictions of the mathematical model

3.2.1 The relationship between K_d and RLU is not intuitive

Although the observed luminescence (RLU) is correlated to the degree of interaction between the protein pair of interest, it has been unknown how direct this correlation is. The relationship between changes of the affinity of a protein pair and observed luminescence was analyzed using the mathematical model.

The model suggests that the relationship between the K_d (the affinity of a protein pair) and the RLU is exponentially rather than linearly correlated (Fig. 3.8). To obtain this data, protein pair affinities were varied over 24 different values, from 2.5 nM to 3 μM. The k_{on} was held constant at a physiologically relevant $1 \cdot 10^6 M^{-1}s^{-1}$ and the maximum RLU was plotted [29]. This simulation demonstrates that the FLCA luminesence can be misleading about the affinity of the protein pair. For example, when comparing the maximum RLU at K_d 3 μM and .75 μM, the affinity increases 4 fold, but the RLU increases 6 fold (Fig. 3.8(B)). When comparing high affinities, for example 10 nM and 100 nM, the affinity increases 10 fold but the RLU increases 2 fold (Fig. 3.8(C)). This suggests that the FLCA would be extremely misleading when considering protein pairs with very high affinity, but more accurate for protein pairs with lower affinity.

Predicted effect of K_d on the kinetics of the FLCA The model predicts that the peak RLU duering the FLCA assay decreases with the affinity of the protein pair fused to NFLuc and CFLuc (Fig. 3.9). To simulate this relationship, protein pair affinities were varied over 24 different values, from 2.5 nM to 3 μM. The k_{on} was held constant at a physiologically relevant $1 \cdot 10^6 M^{-1}s^{-1}$ and the kinetics were plotted for 100 s [29]. As the K_d decreases, the kinetics shift from having a sharp peak RLU and consequent decay, to being nearly flat.

It is not unreasonable to look for a luminesence signal that is above background to identify the presence of a protein-protein interaction when using the FLCA. For protein pairs above 1 μM, the peak RLU is predicted to be very flat and low in magnitude, such that it may appear to be a non-interacting pair (Fig. 3.9(A)).

In Fig. 3.9(A), the concentration of NFLuc and CFLuc were held constant at 50 nM each. This is significantly below the K_d of the very low affinity protein pairs which might appear to be non-interacting (i.e. 1 μM and above). To observe the effect of a more appropriate concentration for this affinity range, the concentration was raised to 1 μM in Fig. 3.9(B). This improved peak definition in the lower K_d range, but did not completely solve

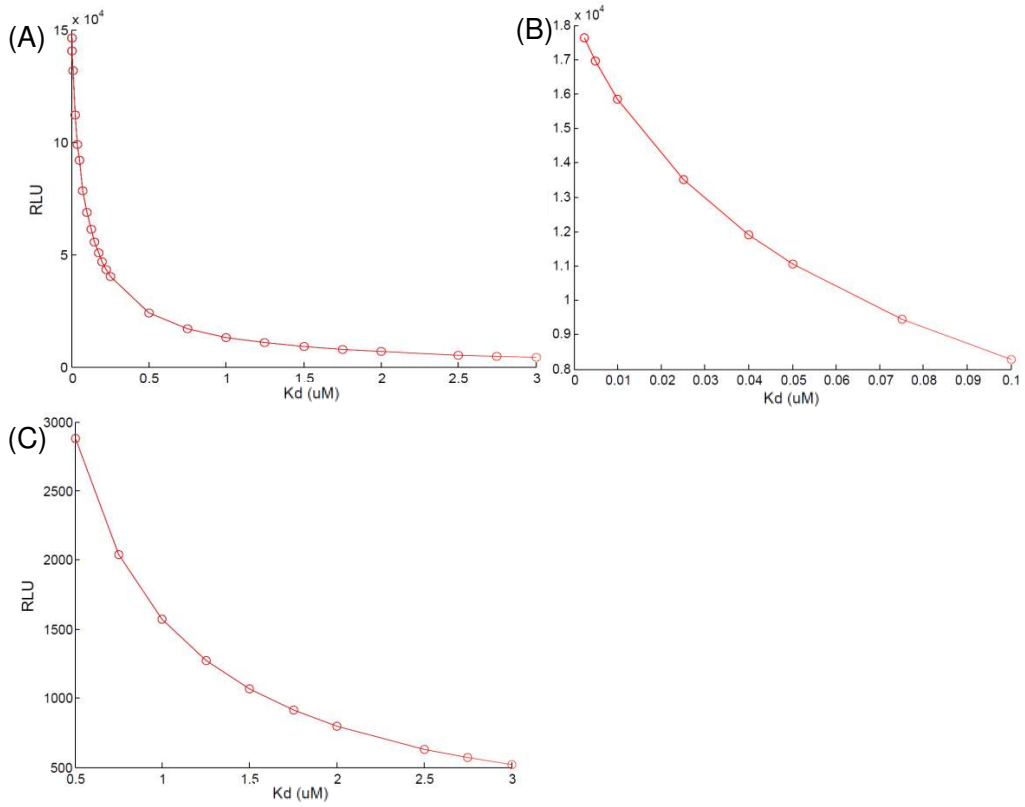

Figure 3.8: Directly comparing RLU obtained by the FLCA with different protein pairs may cause misunderstandings about their affinities. (A) The model predicts an exponential relationship between changes of K_d and maximum RLU. (B) For protein pairs that have low K_d (i.e., K_d varied between 2.5-100 nM), comparing RLU underestimates changes of the affinity. An RLU twice as high correlates with K_ds 10 times as high. (C) For protein pairs that have high K_d (i.e., K_d is between 0.5-3 μM), the changes in RLU are somewhat closer to changes in K_d. An RLU twice as high correlates with a K_d 1.5 times higher.

the issue. When the concentration of NFLuc and CFLuc is increased in this manner, the peak RLU for higher affinity protein pairs begins to cluster more tightly. For such assay conditions, directly comparing protein pairs of different affinities must be qualitative.

These findings raise a question of the validity of the previous interpretation of the FLCA conducted in the past. Some previous papers claim that the RLU and the K_d are linear [41, 51]. Even when we assume that *in vitro* and *in vivo* reaction conditions are identical, the RLU detected underestimates the K_d of a protein pair. It is conceivable that experimental errors occur more often *in vivo* than *in vitro*. It is also conceivable that reaction conditions *in vitro* and *in vivo* are largely different [68]. Therefore, we suggest that the FLCA data published in the past were qualitative assays if the RLU of a protein pair was directly compared to another protein pair.

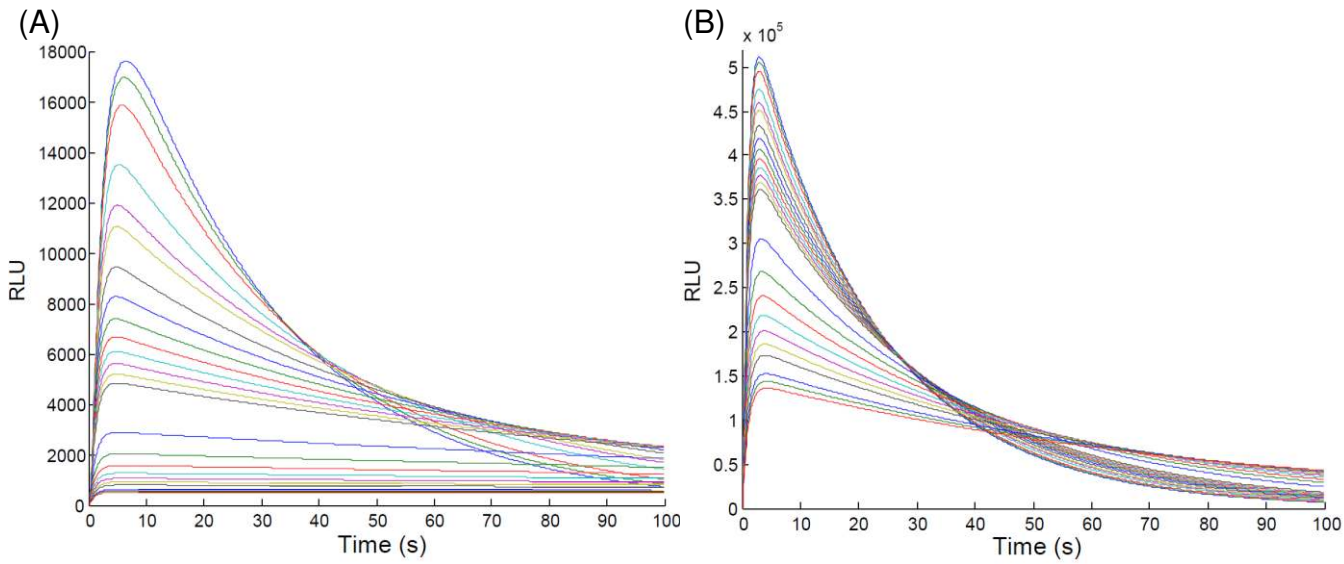

Figure 3.9: Model predicts that peak definition decreases as K_d increases. The model was solved for 24 K_ds which were from 2.5 nM to 3 μM and the kinetics were plotted over 100 s. Each subsequent K_d is plotted in a different color. (A) The model suggests that as the K_d decreases, the peak definition is slowly lost, to the point of appearing flat and steady. For high K_ds, such as 1 to 3 μM, the luminesence may be confused with the background. (B) Increasing the concentration of enzyme from 50 nM to 1 μM causes more defined peaks in low K_d pairs, but less difference between peaks.

3.2.2 Suggested *in vitro* experimental design for quantitative FLCA

The model created in this study can aid in the design of an *in vitro* experiment to obtain the K_d for a protein pair of interest. We suggest to obtain a satruation binding curve using increasing titrations of CFLuc. This will enable the identification of the 50% binding point, or the K_d, using nonlinear curve fitting to the data set using equation 3.4 [29]. The feasibility of this *in vitro* is demonstrated by the IC-50 curve results, as this is another type of saturation curve.

We suggest titrating a protein fused to CFLuc over a large series of concentrations while using a constant, minimal concentration of a protein fused to NFLuc [29]. The lower the concentration of NFLuc, the less CFLuc is needed to fully saturate NFLuc. The concentrations of LH_2 and ATP should be kept at a constant, saturating level during the experiment. Then the maximum RLU observed during the assay for each different concentration of CFLuc added should be collected. To ensure that NFLuc is completely bound, we suggest that the same maximum RLU should be obtained with two separate concentrations of CFLuc. A loss in accuracy is to be expected if 0% and 100% bound NFLuc are not measured [29, 90].

The K_d can be then calculated by nonlinear regression to a quadratic formula which expresses the relationship between binding and K_d (Eqn. 3.4) [29]. The simulation results are shown in Fig. 3.10. For this simulation, the K_d of the protein pair was set to 100 nM and the k_{on} was set at $1{\cdot}10^6 M^{-1}s^{-1}$ [29]. The concentration of NFLuc was set to 1 nM, and 20

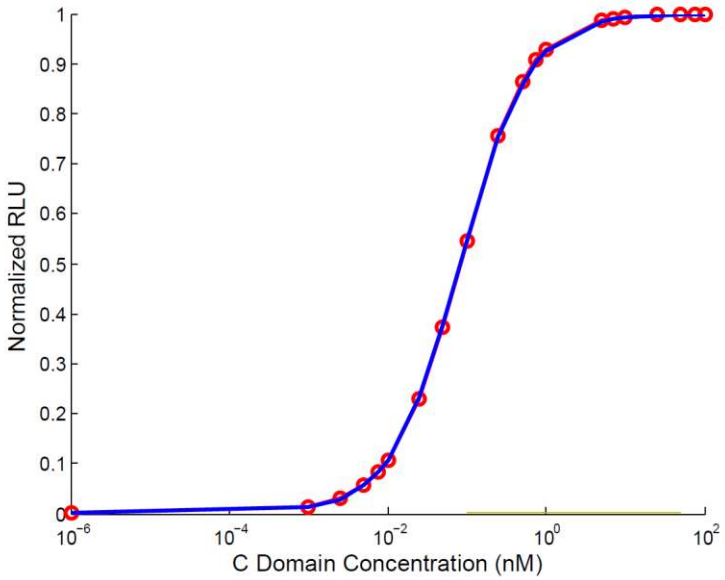

Figure 3.10: The K_d can be obtained by the FLCA *in vitro* by nonlinear regression (blue) to the saturation curve formed by peak RLU values (red). By titrating CFLuc from $1{\cdot}10^{-3}$ nM to $1{\cdot}10^{3}\mu$M while NFLuc is held at 1 nM, the predefined K_d (shown here, 100 nM) can be reasonably re-obtained at 83 nM. To properly estimate K_d, the same maximum RLU must be obtained multiple times, to establish that NFLuc cannot be bound to any more CFLuc. For a K_d of 100 nM, approximately 100μM is required to accomplish this. After finding the point at which 100% NFLuc is bound to CFLuc, the maximum RLU points are normalized to one. The K_d is calculated using the maximum RLU and linear regression to a quadratic formula described previously [29] to find the concentration of CFLuc required to reach 50% saturation.

different concentrations of a protein fused to CFLuc was varied from 100 pM to $1{\cdot}10^{6}$ nM. 100 pM was used to establish near 0% binding. The maximum RLU was calculated, and linear regression was performed to a quadratic formula describing the relationship between % bound N and K_d (equation 3.4) [29]. Nonlinear regression to this equation provided an estimated K_d of 83 nM. The predicted kinetics of this experiment are shown in Fig. 3.11.

$$\text{Bound N} = \frac{[N] + [C] + K_d - ([N] + [C] + K_d^2 - 4 \cdot [N] \cdot [C]^{0.5})}{2 \cdot [N]} \tag{3.4}$$

The model suggests that a pitfall of this experiment is requirement of high concentrations of CFLuc to complete the titration curve. A complete titration curve requires both values corresponding to 0% and 100% activity [29]. For instance, if one only titrates CFLuc up to 1 μM, 100 times less than the simulated maximum of 100 μM, the estimated K_d obtained via nonlinear regression is 65 nM. If one titrates CFLuc up to 10 μM however, 10 times less than the simulated maximum of 100 μM. the estimated K_d is 81 nM, a small reduction in accuracy.

3.2.3 Conclusion

In this study, we found that the cause of the change in luminescence kinetics between full length and split firefly luciferase is due primarily to decreases in the adenylation and oxidation rates, in addition to the transient nature of the interaction between NFLuc and CFLuc. Branchini et al first demonstrated the effect of the removal of the C terminal domain's catalytic residues by measuring the luminescence production in a recombinant protein [6]. The mathematical model and parameter estimation results agree with previously obtained binding and catalytic values. The model also demonstrates that these kinetic effects cause the relationship between luminescence and the affinity of the protein pair fused to NFLuc and CFLuc to be exponential rather than linear. The model explains that although it is possible to obtain qualitative information of the protein-protein interaction (whether or not the proteins interact) by comparing two sets of FLCA data, the non intuitive relationship between RLU and K_d of a protein pair prevents such comparisons from being quantitative. The simulations demonstrates that the FLCA can be used to obtain quantitative information about the protein pair of interest if a large range of titration experiments are conducted to obtain a saturation curve.

Although the FLCA is a convenient and cost-effective assay to analyze protein-protein interactions both *in vitro* and *in vivo*, utilizing the FLCA as a quantitative assay remains a challenge. One of the most challenging aspects is to understand how the "active site" of firefly luciferase is reconstituted when the proteins fused to NFLuc and CFLuc interact. It is known that when NFLuc and CFLuc are fused to different locations of a protein pair (.i.e., amino- or carboxyl- terminal end of proteins of interest), the RLU observed in the FLCA assay varies greatly [28]. This shows that the geometry of NFLuc and CFLuc in the interacting protein complex can largely influence how the active site is reconstituted. This phenomenon particularly demonstrates how directly comparing RLU between protein pairs must be considered qualitative. Although the geometry of the interacting protein complex will vary depending on the proteins of interest and the recombinant areas, it seems reasonable that the geometry of NFLuc and CFLuc in the interacting protein complex would not change significantly based on different environmental conditions (such as pH, the presence of small compounds, etc). Accordingly, one may assume that the FLCA can be used to compare the quantitatively obtained K_ds directly, regardless of different environmental conditions. However the I model created in this thesis explains that obtaining the K_d of a protein pair requires a saturation curve, regardless of the environmental or geometric conditions.

FLCA is thought to be most useful *in vivo* [68]. However, because expressing large concentrations of proteins *in vivo* is not always feasible, the quantitative FLCA (i.e., determining K_d of a protein pair) may not be feasible for *in vivo* with the current experimental design. The identification of k_{on} and k_{off} *in vitro* afford another challenge. Identification of the k_{on} would be relatively simple, using the same method as described for the measurement of the K_d. Measuring the k_{off} must require further experimental design, however, as it requires the addition of competing proteins during the kinetic reaction. Since luciferase is inhibited by its products, such an experiment would require either math modeling to aid in data interpretation, or the use of a different system that does not experience product inhibition. The future goal of this project is to analyze the suitability of the quantitative

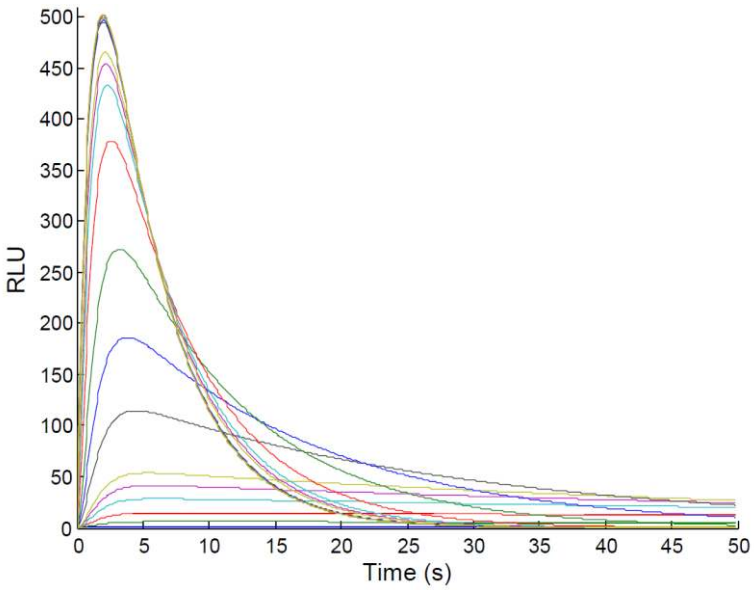

Figure 3.11: Predicted kinetics upon the titration of CFLuc to a constant level of NFLuc. CFLuc was titrated with 20 different concentrations, varying from 100 pM to $1{\cdot}10^6$ nM. The model shows that as the concentration of CFLuc increases, the peak will become more and more defined, until it reaches some maximum. Each subsequent simulation is plotted in a different color. 100 pM of CFLuc lies on the x-axis and $75{\cdot}10^5$ and $1{\cdot}10^6$ nM overlap to form the highest peak.

FLCA for the measurement of the k_{off}, as well as the suitability of the quantitative FLCA for *in vivo* applications.

Chapter 4
Materials and Methods

4.1 Materials and Methods

4.1.1 Experimental

Measurement of the kinetics of full length firefly luciferase Full length firefly luciferase data was collected under similar conditions as in [28]. Briefly, ATP and LH_2 were purchased from Thermo Scientific (Rockford, IL). MOPS was from Acros Organics (Thermo Fisher Scientific, Geel, Belgium). Firefly luciferase was purchased from Promega (Wisconsin, USA). Luciferase enzyme was suspended in 100 mM MOPS, 19 mM $MgSO_4$, pH 7.3. 1 μL of the enzyme solution and 50 μL of a 2x ATP solution (40 mM ATP in 100 mM MOPS, 10 mM $MgSO_4$, pH 7.3) was dispensed to a well in a white 96-well plate (Corning-Costar, NY, USA). The luminescence was measured immediately after injection of a 2x LH_2 solution (150 μM LH_2, 100 mM MOPS, 10 mM $MgSO_4$, pH 7.3) with periodical integration for 0.2 s for 120 s using Synergy 2 luminometer (Biotek, Vermont, USA).

4.1.2 Calculations

Calculation of the degradation of split firefly luciferase. Degradation analysis due to heat inactivation was performed previously [28]. The maximum RLU for each incubation time was digitized using PlotDigitizer and normalized [16]. The degradation rate was calculated by curve fitting an equation describing exponential degradation 3.1. The curve fit was accomplished using Matlab's nlinfit function for nonlinear equations [26].

Estimation of parameters Initial estimates for parameters were taken from the literature (Table 1.1). Initial estimates for all k_{on} rates were held between the physiologically relevant range of $10^5 - 10^8 M^{-1}$ [29]. Parameters unavailable from the literature were estimated by curve fitting the model to previous data. The parameters we needed to estimate were the adenylation rates, and the dark reaction frequency. Previous data suggests relative adenylation rates [6], but no forward or reverse rate estimates were available. Measuring the adenylation rate directly is a technical challenge as its product is pyrophosphate and enzyme bound to the intermediate [6]. Previous mutagenesis data suggested an increase in dark reaction frequency but the exact value is unknown [25, 6].

To estimate these values, NFLuc only data was digitized from previously published data using PlotDigitizer [3, 16]. The mathematical model (ODE 2.1.3) was modified to remove all references to CFLuc and the NC complex prior to curve fitting (ODE 4.1.2). Curve fitting to the luminescence kinetics obtained when LH_2 and ATP were added provided estimates for the adenylation rates and dark reaction frequency. The curve fit to the luminescence kinetics obtained with the addition of LH_2-AMP alone provided improved estimates for the oxidation rate and intermediate affinity.

Functions utilized by the model The ODE was solved with MatLab's ode23s for stiff systems [26]. Our ODEs were determined stiff by the relative computation time to solve

the ODEs. ode45 took several minuts, while ode23s took only 1.4 seconds to solve the entire system of ODEs. ode23s solves the differential equations over a defined timespan with defined timesteps. Our timespan and timesteps was defined by the data set. A vector of initial conditions is supplied to provide starting values for the calculations.

The curve fitting was done using MatLab's lsqcurvefit function. lsqcurvefit optimizes an input vector of parameters by calculating the squared difference between the model output and the data. It then changes the values of parameters by small increments until improvement is made upon this squared difference. The parameters are kept within user-defined numeric boundaries, supplied to the lsqcurvefit function in the form of vectors.

The calculation of IC-50 and K_d values were accomplished using nlinfit in Matlab [26]. For the specified nonlinear function, nlinfit calculates best-ft values for variables contained within the function. nlinfit uses an iterative reweighted least squares algorithm to optimize the values given vectors containing the observed data values and the input values (such as time). The weights given to a parameter within the function are recalculated with each successive iteration.

Calculation of initial conditions The model calculates the initial concentrations of non-interacting and interacting protein pair prior to running a simulation. This is calculated using the k_{on} and k_{off} for the protein pair, the initial concentration of the proteins, the degradation rate of split firefly luciferase, and the incubation time with the system of equations shown in Appendix C (ODE C1). The k_{on} and k_{off} of the protein pair was obtained from a previous paper [31]. The initial concentration of the proteins was determined experimentally. The incubation time was approximated at 1 s due to delays of the substrate injection by the machine if no incubation time was defined by the experimenters. The degradation rate was calculated by curve fitting to previously obtained data [28]. FLCA proteins were incubated at 37 ℃ for 0 to 60 minutes and the resulting activity monitored. The maximum RLU was obtained from this data using PlotDigitizer. The maximum RLU at 0 minutes incubation was assumed to represent 100% activity.

Curve fit After obtaining parameter estimates for NFLuc alone, estimates for NC complex binding and catalysis rates were taken from the literature. The system of ODE was curve fit using lsqcurvefit to data obtained by our collaborators in this project. The effect of the light sensor (photomultiplier tube) was negated by normalizing data and model simulations. In most cases the peak will be the maximum RLU of a data set. However, in the long term data set, a few outliers can be observed which causes normalization to be non ideal. For this data set, therefore, the magnification effect of the photomultiplier tube was optimized as well. After obtaining the parameters, the model was compared to previously published p53-mdm2 data under various concentrations [28]. To eliminate variations due to the photomultiplier tube, the data and model output were normalized.

ODE 4.1.2

Stripped-down ODEs describing the binding and catalysis interactions of NFLuc only

$$\frac{dx_1}{dt} = -c_9 \cdot x_1 \cdot x_6 + c_{10} \cdot x_{16} - c_7 \cdot x_1 \cdot x_3 + c_8 \cdot x_{15} - c_{24} \cdot x_1 \cdot x_{14} + c_{25} \cdot x_{19}$$
$$- c_{26} \cdot x_1 \cdot x_{12} + c_{27} \cdot x_{20} - c_{15} \cdot x_1 \cdot x_9 + c_{16} \cdot x_{18}$$
$$\frac{dx_3}{dt} = -c_7 \cdot x_1 \cdot x_3 + c_8 \cdot x_{15} - c_7 \cdot x_{16} \cdot x_3 + c_8 \cdot x_{17}$$
$$\frac{dx_6}{dt} = -c_9 \cdot x_1 \cdot x_6 + c_{10} \cdot x_{16} - c_9 \cdot x_{15} \cdot x_6 + c_{10} \cdot x_{17}$$
$$\frac{dx_9}{dt} = -c_{15} \cdot x_2 \cdot x_9 + c_{16} \cdot x_8 - c_{15} \cdot x_1 \cdot x_9 + c_{16} \cdot x_{18}$$
$$\frac{dx_{12}}{dt} = -c_{21} \cdot x_2 \cdot x_{12} + c_{22} \cdot x_{11} - c_{26} \cdot x_1 \cdot x_{12} + c_{27} \cdot x_{20}$$
$$\frac{dx_{13}}{dt} = -x_{13} + c_{17} \cdot x_{18} \cdot (1 - c_{23}) \cdot c_{19}$$
$$\frac{dx_{14}}{dt} = -c_{24} \cdot x_1 \cdot x_{14} + c_{25} \cdot x_{19}$$
$$\frac{dx_{15}}{dt} = c_7 \cdot x_1 \cdot x_3 - c_8 \cdot x_{15} - c_9 \cdot x_{15} \cdot x_6 + c_{10} \cdot x_{17}$$
$$\frac{dx_{16}}{dt} = c_9 \cdot x_1 \cdot x_6 - c_{10} \cdot x_{16} - c_7 \cdot x_{16} \cdot x_3 + c_8 \cdot x_{17}$$
$$\frac{dx_{17}}{dt} = -c_{13} \cdot x_{17} + c_{14} \cdot x_{18} + c_9 \cdot x_{15} \cdot x_6 - c_{10} \cdot x_{17} + c_7 \cdot x_{16} \cdot x_3 - c_8 \cdot x_{17}$$
$$\frac{dx_{18}}{dt} = c_{13} \cdot x_{17} - c_{14} \cdot x_{18} - c_{17} \cdot x_{18} + c_{15} \cdot x_1 \cdot x_9 - c_{16} \cdot x_{18}$$
$$\frac{dx_{19}}{dt} = c_{17} \cdot (1 - c_{23}) \cdot x_{18} + c_{24} \cdot x_1 \cdot x_{14} - c_{25} \cdot x_{19}$$
$$\frac{dx_{20}}{dt} = c_{17} \cdot c_{23} \cdot x_{18} + c_{26} \cdot x_1 \cdot x_{12} - c_{27} \cdot x_{20}$$

Simulation of inhibition To simulate the inhibition of p53 and mdm2 by nutlin-3, as performed in [28], the model (ODE 2.1.3) was modified to reflect a three-way molecular interaction (ODE C2, appendix C). The initial concentrations were calculated prior to the simulation as the previous paper described an incubation step [28]. The initial conditions for this three-way interaction were calculated using ODE C3 (See appendix C). The experiment used 100 nM of NFLuc and CFLuc with concentrations of nutlin-3 varying from 1 nM to 16 μM. The experimental values were taken at 0.2 s. To calculate the IC-50, the RLU at 0.2 s were plotted and the IC-50 values were calculated. These points were fit using nonlinear regression to equation 3.3. Nonlinear regression and plotting was accomplished using a modified form of the independently designed DoseResponse package for Matlab [40]. The default equation for the DoseResponse package was changed to reflect the goals of the curve fit.

Relationship of RLU to K_d To examine the relationship between the maximum RLU and the K_d of the attached protein pair, a range of 24 K_ds were used, with the value varied from 2.5 nM to 3 μM. The k_{on} was held constant at $1{\cdot}10^7 M^{-1}s^{-1}$ [29]. Initial concentra-

tions of p53 and mdm2 fusing to NFLuc and CFLuc, respectively, were 50 nM each. The maximum RLUs were compared.

Prediction of K_d To determine the ability of the FLCA to detect the K_d of the attached protein pair, the concentration of CFLuc was varied from $1 \cdot 10^{-3}$ nM to $1 \cdot 10^{6}$ nM while the concentration of NFLuc was held constant at 1 nM. This range was determined by ensuring the maximum RLU could not be increased by increasing the protein fused to CFLuc. This was determined by obtaining the maximum RLU multiple times. The maximum RLU of each CFLuc concentration was plotted, and the highest RLU was considered 100% bound NFLuc. These points were fit using nonlinear regression to equation 3.4 [29].

To determine K_d, the equation was solved using nonlinear regression for the concentration of the protein fused to CFLuc corresponding to 50% bound NFLuc. Nonlinear regression was accomplished using Matlab's nlinfit function. The resulting estimated K_d was compared to the K_d defined for the interaction between the simulated protein pair fused to the NFLuc and CFLuc, respectively.

References

[1] Arkin, M. R. & Wells, J. A. Small-molecule inhibitors of proteinprotein interactions: progressing towards the dream. Nature Reviews Drug Discovery 3, 301317 (2004).

[2] Auld DS, Southall NT, Jadhav A, Johnson RL, Diller DJ, Simeonov A, et al. Characterization of Chemical Libraries for Luciferase Inhibitory Activity. Journal of Medicinal Chemistry. 2008 Apr;51(8):237286.

[3] Ayabe, K., Zako, T. & Ueda, H. The role of firefly luciferase C-terminal domain in efficient coupling of adenylation and oxidative steps. FEBS Letters 579, 43894394 (2005).

[4] Braeuning A. Firefly luciferase inhibition: a widely neglected problem. Archives of Toxicology. 2015 Jan;89(1):1412.

[5] Banaszynski LA, Liu CW, Wandless TJ. Characterization of the FKBP-Rapamycin-FRB Ternary Complex. Journal of the American Chemical Society. 2005 Apr;127(13):471521.

[6] Branchini BR, Southworth TL, Murtiashaw MH, Wilkinson SR, Khattak NF, Rosenberg JC, et al. Mutagenesis Evidence that the Partial Reactions of Firefly Bioluminescence Are Catalyzed by Different Conformations of the Luciferase C-Terminal Domain. Biochemistry. 2005 Feb;44(5):138593.

[7] Branchini BR, Southworth TL, Murtiashaw MH, Boije H, Fleet SE. A Mutagenesis Study of the Putative Luciferin Binding Site Residues of Firefly Luciferase. Biochemistry. 2003 Sep;42(35):1042936.

[8] Branchini BR, Murtiashaw MH, Magyar RA, Anderson SM. The Role of Lysine 529, a Conserved Residue of the Acyl-Adenylate-Forming Enzyme Superfamily, in Firefly Luciferase. Biochemistry. 2000 May;39(18):543340.

[9] Conti E, Franks NP, Brick P. Crystal structure of firefly luciferase throws light on a superfamily of adenylate-forming enzymes. Structure. 1996;4(3):28798.

[10] Pinto da Silva, L., Vieira, J. & Esteves da Silva, J. C. G. Comparative theoretical study of the binding of luciferyl-adenylate and dehydroluciferyl-adenylate to firefly luciferase. Chemical Physics Letters 543, 137141 (2012).

[11] Da Silva LP, Esteves da Silva JCG. Computational Studies of the Luciferase Light-Emitting Product: Oxyluciferin. Journal of Chemical Theory and Computation. 2011 Apr 12;7(4):80917.

[12] Da Silva, L. P. & Esteves da Silva, J. C. G. Kinetics of inhibition of firefly luciferase by dehydroluciferyl-coenzyme A, dehydroluciferin and l-luciferin. Photochemical & Photobiological Sciences 10, 1039 (2011).

[13] Gates, B. J. & DeLuca, Marlene. The Production of Oxyluciferin During the Firefly Luciferase Light Reaction. Archives of Biochemistry and Biophysics 159, 616621 (1975).

[14] Hulme EC, Trevethick MA. Ligand binding assays at equilibrium: validation and interpretation. British journal of pharmacology. 2010;161(6):121937.

[15] Humphrey, W., Dalke, A. and Schulten, K., "VMD - Visual Molecular Dynamics", J. Molec. Graphics, 1996, vol. 14, pp. 33-38. http://www.ks.uiuc.edu/Research/vmd/

[16] Huwaldt, Joseph A. Plot Digitizer. http://sourceforge.net/projects/plotdigitizer/

[17] Ignowski JM, Schaffer DV. Kinetic analysis and modeling of firefly luciferase as a quantitative reporter gene in live mammalian cells. Biotechnol Bioeng. 2004 Jun 30 86(7):827-34. p.830

[18] Laurie NA, Donovan SL, Shih C-S, Zhang J, Mills N, Fuller C, et al. Inactivation of the p53 pathway in retinoblastoma. Nature. 2006 Nov 2;444(7115):616.

[19] Leito, J. M. M. & Esteves da Silva, J. C. G. Firefly luciferase inhibition. Journal of Photochemistry and Photobiology B: Biology 101, 18 (2010).

[20] Lembert, N. & Idahl, L.-A. Regulatory effects of ATP and luciferin on firefly luciferase activity. Biochem. J 305, 929933 (1995).

[21] Li J-F, Bush J, Xiong Y, Li L, McCormack M. Large-Scale Protein-Protein Interaction Analysis in Arabidopsis Mesophyll Protoplasts by Split Firefly Luciferase Complementation. PLoS ONE. 2011 Nov 9;6(11):e27364.

[22] Luker KE, Steele JM, Mihalko LA, Ray P, Luker GD. Constitutive and chemokine-dependent internalization and recycling of CXCR7 in breast cancer cells to degrade chemokine ligands. Oncogene. 2010;29(32):4599610.

[23] Luker KE, Smith MCP, Luker GD, Gammon ST, Piwnica-Worms H, Piwnica-Worms D. Kinetics of regulated proteinprotein interactions revealed with firefly luciferase complementation imaging in cells and living animals. Proc Natl Acad Sci U S A. 2004 Aug 17;101(33):1228893.

[24] Manninen T, Ribeiro A, Lloyd-Price J, Linne M-L, Ruohonen K, Yli-Harja O, et al. Parameter estimation and tuning of firefly luciferase pathway model. Genomic Signal Processing and Statistics, 2007 GENSIPS 2007 IEEE International Workshop on [Internet]. IEEE; 2007 [cited 2015 Jun 11]. p. 14.

[25] Marques, S. M. & Esteves da Silva, J. C. G. Firefly bioluminescence: A mechanistic approach of luciferase catalyzed reactions. IUBMB Life 61, 617 (2009).

[26] MATLAB Release 2014a, The MathWorks, Inc., Natick, Massachusetts, United States.

[27] Laurie NA, Donovan SL, Shih C-S, Zhang J, Mills N, Fuller C, et al. Inactivation of the p53 pathway in retinoblastoma. Nature. 2006 Nov 2;444(7115):616.

[28] Ohmuro-Matsuyama, Y., Chung, C.-I. & Ueda, H. Demonstration of protein-fragment complementation assay using purified firefly luciferase fragments. BMC biotechnology 13, 31 (2013).

[29] Pollard TD. A Guide to Simple and Informative Binding Assays. Molecular Biology of the Cell. 2010 Dec 1;21(23):40617.

[30] Ribeiro, C. & Esteves da Silva, J. C. G. Kinetics of inhibition of firefly luciferase by oxyluciferin and dehydroluciferyl-adenylate. Photochemical & Photobiological Sciences 7, 1085 (2008).

[31] Schon, O., Friedler, A., Bycroft, M., Freund, S. M. & Fersht, A. R. Molecular Mechanism of the Interaction between MDM2 and p53. Journal of Molecular Biology 323, 491501 (2002).

[32] Sundlov JA, Fontaine DM, Southworth TL, Branchini BR, Gulick AM. Crystal Structure of Firefly Luciferase in a Second Catalytic Conformation Supports a Domain Alternation Mechanism. Biochemistry. 2012 Aug 21;51(33):64935.

[33] Thorne, N. et al. Firefly Luciferase in Chemical Biology: A Compendium of Inhibitors, Mechanistic Evaluation of Chemotypes, and Suggested Use As a Reporter. Chemistry & Biology 19, 10601072 (2012).

[34] Thorne, N., Inglese, J. & Auld, D. S. Illuminating Insights into Firefly Luciferase and Other Bioluminescent Reporters Used in Chemical Biology. Chemistry & Biology 17, 646657 (2010).

[35] Tseng C-Y, Zocchi G. Mechanical Control of Renilla Luciferase. Journal of the American Chemical Society. 2013 Aug 14;135(32):1187986.

[36] Vassilev LT, Vu BT, Graves B, Carvajal D, Podlanski F, Filipovic Z, Kong N, Kammlott Ursula, Lukacs C, Klein C, Fotouhi N, Liu EA. In Vivo Activation of P53 pathway by Small -Molecule Antagonists of MDM2. Science. 2004 Feb 6;303(5659):844-8.

[37] Woo J, von Arnim AG. Mutational optimization of the coelenterazine-dependent luciferase from Renilla. Plant Methods. 2008;4(1):23.

[38] Zako, T. et al. Luminescent and substrate binding activities of firefly luciferase N-terminal domain. Biochimica et Biophysica Acta (BBA) - Proteins and Proteomics 1649, 183189 (2003).

[39] Zhu Y, Wang Y, Li R, Song X, Wang Q, Huang S, et al. Analysis of interactions among the CLAVATA3 receptors reveals a direct interaction between CLAVATA2 and CORYNE in Arabidopsis: Direct interaction between CLAVATA2 and CORYNE. The Plant Journal. 2009 Nov 5;61(2):22333.

[40] http://www.mathworks.com/matlabcentral/fileexchange/33604-doseresponse

[41] Chen H, Zou Y, Shang Y, Lin H, Wang Y, Cai R, et al. Firefly Luciferase Complementation Imaging Assay for Protein-Protein Interactions in Plants. PLANT PHYSIOLOGY. 2007 Dec 7;146(2):36876.

[42] Coppola JM, Ross BD, Rehemtulla A. Noninvasive Imaging of Apoptosis and Its Application in Cancer Therapeutics. Clinical Cancer Research. 2008 Mar 27;14(8):2492501.

[43] Deng K, Li X, Wang Q, Zeng J, Zhao X, Tang D, et al. Lectin receptor kinase LecRK-b2 localizes to plasma membrane and functions as a homdimer. African Journal of Biotechnology [Internet]. 2009 [cited 2015 May 4];8(14). Available from: http://www.ajol.info/index.php/ajb/article/view/61043

[44] Endoh T, Mie M, Funabashi H, Sawasaki T, Endo Y, Kobatake E. Construction of Intramolecular Luciferase Complementation Probe for Detecting Specific RNA. Bioconjugate Chemistry. 2007 May;18(3):95662.

[45] Fujikawa Y, Kato N. TECHNICAL ADVANCE: Split luciferase complementation assay to study proteinprotein interactions in Arabidopsis protoplasts. The Plant Journal. 2007 Oct 1;52(1):18595.

[46] Hashimoto T, Adams KW, Fan Z, McLean PJ, Hyman BT. Characterization of Oligomer Formation of Amyloid- Peptide Using a Split-luciferase Complementation Assay. Journal of Biological Chemistry. 2011 Aug 5;286(31):2708191.

[47] Hsu W-C, Nenov MN, Shavkunov A, Panova N, Zhan M, Laezza F. Identifying a Kinase Network Regulating FGF14: Nav1. 6 Complex Assembly Using Split-Luciferase Complementation. PLOS ONE Feb 6; 10 (2): e0117246 doi [Internet]. 2015 [cited 2015 May 4];10. Available from: http://dx.plos.org/10.1371/journal.pone.0117246

[48] Kim H-K, Cho EJ, Jo S mi, Sung BR, Lee S, Yun S-H. A split luciferase complementation assay for studying in vivo proteinprotein interactions in filamentous ascomycetes. Current Genetics. 2012 Jun;58(3):17989.

[49] Kimura M, Murakami T, Kizaka-Kondoh S, Itoh M, Yamamoto K, Hojo Y, et al. Functional molecular imaging of ILK-mediated Akt/PKB signaling cascades and the associated role of -parvin. Journal of Cell Science. 2010 Mar 1;123(5):74755.

[50] Krycer JR, Brown AJ. Cross-talk between the Androgen Receptor and the Liver X Receptor: IMPLICATIONS FOR CHOLESTEROL HOMEOSTASIS. Journal of Biological Chemistry. 2011 Jun 10;286(23):2063747.

[51] Li J-F, Bush J, Xiong Y, Li L, McCormack M. Large-Scale Protein-Protein Interaction Analysis in Arabidopsis Mesophyll Protoplasts by Split Firefly Luciferase Complementation. PLoS ONE. 2011 Nov 9;6(11):e27364.

[52] Li L, Li M, Yu L, Zhou Z, Liang X, Liu Z, et al. The FLS2-Associated Kinase BIK1 Directly Phosphorylates the NADPH Oxidase RbohD to Control Plant Immunity. Cell Host & Microbe. 2014 Mar;15(3):32938.

[53] Li W, Yadeta KA, Elmore JM, Coaker G. The Pseudomonas syringae Effector HopQ1 Promotes Bacterial Virulence and Interacts with Tomato 14-3-3 Proteins in a Phosphorylation-Dependent Manner. PLANT PHYSIOLOGY. 2013 Apr 1;161(4):206274.

[54] Luker KE, Steele JM, Mihalko LA, Ray P, Luker GD. Constitutive and chemokine-dependent internalization and recycling of CXCR7 in breast cancer cells to degrade chemokine ligands. Oncogene. 2010;29(32):4599610.

[55] Moisy D, Avilov SV, Jacob Y, Laoide BM, Ge X, Baudin F, et al. HMGB1 Protein Binds to Influenza Virus Nucleoprotein and Promotes Viral Replication. Journal of Virology. 2012 Sep 1;86(17):912233.

[56] Morsy M, Gouthu S, Orchard S, Thorneycroft D, Harper JF, Mittler R, et al. Charting plant interactomes: possibilities and challenges. Trends in Plant Science. 2008 Apr;13(4):18391.

[57] Nyati S, Ross BD, Rehemtulla A, Bhojani MS. Novel molecular imaging platform for monitoring oncological kinases. Cancer Cell Int. 2010;10:23.

[58] Ramkumar KM, Sekar TV, Foygel K, Elango B, Paulmurugan R. Reporter Protein Complementation Imaging Assay to Screen and Study Nrf2 Activators in Cells and Living Animals. Analytical Chemistry. 2013 Aug 6;85(15):75429.

[59] Ray P, Lewin SA, Mihalko LA, Lesher-Perez S, Takayama S, Luker KE, et al. Secreted CXCL12 (SDF-1) forms dimers under physiological conditions. Biochemical Journal. 2012 Mar 1;442(2):43342.

[60] Wang M, Yuan F, Hao H, Zhang Y, Zhao H, Guo A, et al. BolOST1, an ortholog of Open Stomata 1 with alternative splicing products in Brassica oleracea, positively modulates drought responses in plants. Biochemical and Biophysical Research Communications. 2013 Dec;442(3-4):21420.

[61] Willmann JK, van Bruggen N, Dinkelborg LM, Gambhir SS. Molecular imaging in drug development. Nature Reviews Drug Discovery. 2008 Jul;7(7):591607.

[62] Xie CG, Lin H, Deng XW, Guo Y. Roles of SCaBP8 in salt stress response. Plant Signaling & Behavior. 2009 Oct;4(10):9568.

[63] Xiong Y, Sheen J. Rapamycin and Glucose-Target of Rapamycin (TOR) Protein Signaling in Plants. Journal of Biological Chemistry. 2012 Jan 20;287(4):283642.

[64] Zhu Y, Wang Y, Li R, Song X, Wang Q, Huang S, et al. Analysis of interactions among the CLAVATA3 receptors reveals a direct interaction between CLAVATA2 and CORYNE in Arabidopsis: Direct interaction between CLAVATA2 and CORYNE. The Plant Journal. 2009 Nov 5;61(2):22333.

[65] Aelvoet S-A, Ibrahimi A, Macchi F, Gijsbers R, Van den Haute C, Debyser Z, et al. Noninvasive Bioluminescence Imaging of -Synuclein Oligomerization in Mouse Brain Using Split Firefly Luciferase Reporters. Journal of Neuroscience. 2014 Dec 3;34(49):1651832.

[66] Aouida M, Kim K, Shaikh AR, Pardo JM, Eppinger J, Yun D-J, et al. A Saccharomyces cerevisiae Assay System to Investigate Ligand/AdipoR1 Interactions That Lead to Cellular Signaling. Ling MT, editor. PLoS ONE. 2013 Jun 7;8(6):e65454.

[67] Azad T, Tashakor A, Rahmati F, Hemmati R, Hosseinkhani S. Oscillation of apoptosome formation through assembly of truncated Apaf-1. European Journal of Pharmacology. 2015 Aug;760:6471.

[68] Chen H, Zou Y, Shang Y, Lin H, Wang Y, Cai R, et al. Firefly Luciferase Complementation Imaging Assay for Protein-Protein Interactions in Plants. PLANT PHYSIOLOGY. 2007 Dec 7;146(2):36876.

[69] Close DM, Xu T, Sayler GS, Ripp S. In Vivo Bioluminescent Imaging (BLI): Noninvasive Visualization and Interrogation of Biological Processes in Living Animals. Sensors. 2010 Dec 28;11(1):180206.

[70] Gaud G, Guillemot D, Jacob Y, Favre M, Vuillier F. EVER2 protein binds TRADD to promote TNF--induced apoptosis. Cell Death and Disease. 2013 Feb;4(2):e499.

[71] Hee Jin Park, Hyeong Cheol Park, Jida Choi, Wonkyun Choi, Woo Sik Chung, Soohyun Kim, et al. Identification of SUMO-modified Proteins by Affinity Purification and Tandem Mass Spectrometry in Arabidopsis thaliana. J Plant Biol. 2013;56:17685.

[72] Kato N. Luciferase and Bioluminescence Microscopy for Analyses of Membrane Dynamics in Living Cells. Journal of Membrane Science & Technology [Internet]. 2012 [cited 2015 Jun 14];02(03). Available from: http://www.omicsonline.org/2155-9589/2155-9589-2-e109.digital/2155-9589-2-e109.html

[73] Lake MC, Aboagye EO. Luciferase fragment complementation imaging in preclinical cancer studies. Oncoscience. 2014;1(5):310.

[74] Lang Z, Lei M, Wang X, Tang K, Miki D, Zhang H, et al. The Methyl-CpG-Binding Protein MBD7 Facilitates Active DNA Demethylation to Limit DNA Hyper-Methylation and Transcriptional Gene Silencing. Molecular Cell. 2015 Mar;57(6):97183.

[75] Ramiere C, Rodriguez J, Enache LS, Lotteau V, Andre P, Diaz O. Activity of Hexokinase Is Increased by Its Interaction with Hepatitis C Virus Protein NS5A. Journal of Virology. 2014 Mar 15;88(6):324654.

[76] Ray P, Mihalko LA, Coggins NL, Moudgil P, Ehrlich A, Luker KE, et al. Carboxy-terminus of CXCR7 regulates receptor localization and function. The International Journal of Biochemistry & Cell Biology. 2012 Apr;44(4):66978.

[77] Shavkunov AS, Wildburger NC, Nenov MN, James TF, Buzhdygan TP, Panova-Elektronova NI, et al. The Fibroblast Growth Factor 14middle dotVoltage-gated Sodium Channel Complex Is a New Target of Glycogen Synthase Kinase 3 (GSK3). Journal of Biological Chemistry. 2013 Jul 5;288(27):1937085.

[78] Velten J, Pogson B, Cazzonelli CI. Luciferase as a reporter of gene activity in plants. Transgenic Plant J. 2008;2:113.

[79] Zhang L, Virani S, Zhang Y, Bhojani MS, Burgess TL, Coxon A, et al. Molecular imaging of c-Met tyrosine kinase activity. Analytical Biochemistry. 2011 May;412(1):18.

[80] Beyleveld G, White KM, Ayllon J, Shaw ML. New-generation screening assays for the detection of anti-influenza compounds targeting viral and host functions. Antiviral Research. 2013 Oct;100(1):12032.

[81] Dai M, Zhang C, Kania U, Chen F, Xue Q, Mccray T, et al. A PP6-Type Phosphatase Holoenzyme Directly Regulates PIN Phosphorylation and Auxin Efflux in Arabidopsis. The Plant Cell. 2012 Jun;24(6):2497514.

[82] Endo M, Shimizu H, Nohales MA, Araki T, Kay SA. Tissue-specific clocks in Arabidopsis show asymmetric coupling. Nature. 2014 Oct 29;515(7527):41922.

[83] Huang D, Wang S, Zhang B, Shang-Guan K, Shi Y, Zhang D, et al. A Gibberellin-Mediated DELLA-NAC Signaling Cascade Regulates Cellulose Synthesis in Rice. The Plant Cell. 2015 May 22;tpc.15.00015.

[84] Hubbard BP, Loh C, Gomes AP, Li J, Lu Q, Doyle TL, et al. Carboxamide SIRT1 inhibitors block DBC1 binding via an acetylation-independent mechanism. Cell Cycle. 2013 Jul 15;12(14):223340.

[85] Jiang J, Wang B, Shen Y, Wang H, Feng Q, Shi H. The Arabidopsis RNA Binding Protein with K Homology Motifs, SHINY1, Interacts with the C-terminal Domain Phosphatase-like 1 (CPL1) to Repress Stress-Inducible Gene Expression. Chen X, editor. PLoS Genetics. 2013 Jul 11;9(7):e1003625.

[86] Kim H-K, Lee S, Jo S-M, McCormick SP, Butchko RAE, Proctor RH, et al. Functional Roles of FgLaeA in Controlling Secondary Metabolism, Sexual Development, and Virulence in Fusarium graminearum. Yu J-H, editor. PLoS ONE. 2013 Jul 16;8(7):e68441.

[87] Shrestha B, Guragain B, Sridhar VV. Involvement of co-repressor LUH and the adapter proteins SLK1 and SLK2 in the regulation of abiotic stress response genes in Arabidopsis. BMC plant biology. 2014;14(1):54.

[88] Paulmurugan R, Umezawa Y, Gambhir SS. Noninvasive imaging of proteinprotein interactions in living subjects by using reporter protein complementation and reconstitution strategies. Proceedings of the National Academy of Sciences. 2002;99(24):1560813.

[89] McElroy WD, Seliger HH, White EH. MECHANISM OF BIOLUMINESCENCE, CHEMI-LUMINESCENCE AND ENZYME FUNCTION IN THE OXIDATION OF FIREFLY LUCIFERIN*,. Photochemistry and photobiology. 1969;10(3):15370.

[90] Cer RZ, Mudunuri U, Stephens R, Lebeda FJ. IC50-to-Ki: a web-based tool for converting IC50 to Ki values for inhibitors of enzyme activity and ligand binding. Nucleic Acids Research. 2009 Jul 1;37(Web Server):W4415.

[91] Sebaugh JL. Guidelines for accurate EC50/IC50 estimation. Pharmaceutical Statistics. 2011 Mar;10(2):12834.

Appendix A
Matlab Code

```
function main
%%%%%%%%%%%%%%%%%
%%NC parameters
%luciferin
c3=184;
c4=2.999999605697860e+03;

%ATP
c5=30;
c6=4.799990417951311e+03;

%adenylation rate
c11=5.005032362403402e+02;
c12=1.075165513854852e-02;

%kcat
c18=2.186046521866479e-01;

%L-oxy
c19=8.296207031450622e+00;
c20=6.132100294976869e-01;

%L-AMP
c21=5.000500240288718e+01;
c22=2.276804780286590e-05;
%%%%%%%%%%%%%%%%%
%%N domain parameters
%luciferin
c7=1.840621857623435e+02;
c8=5.049917207781118e+03;

%ATP
c9=2.994060619739656e+01;
c10=2.049501880555152e+04;

%adenylation rate
c13=5.496651143939792e-02;
c14=1.100207814311677e-02;

%kcat
c17=3.993565543918900e-07;

%L-oxy N
c24=8.296207031450622e+00;
c25=6.132100294976869e-01;

%L-AMP N
```

```
c26=5.000500240288718e+01;
c27=2.276804780286590e-05;
%%%%%%%%%%%%%%%%%
%%shared parameters
%p53-mdm2
c2=2;
c1=9.2;
kd=.212;

%dark reactions
c23=2.870910570336138e-01;

%intermediate
c15=7.771865248970217e+01;
c16=3.471656490390523e+00;
%%%%%%%%%%%%%%%%%
%degradation during incubation
%c28=.00136;%37 deg heat
c28=0;%no heat
%%%%%%%%%%%%%%%%%
%determine initial concentration
ini_n=.05;
%ini_n=.15;
%ini_n=.45;
ini_c=ini_n;
%incub_time=1;
incub_time=120;
Q=[ini_n;kd;c2;c28;incub_time;ini_c;];
[nconc]=plot_KDp(Q);
initN=nconc(1);
initC=nconc(3);
initNC=nconc(2);
%%%%%%%%%%%%%%%%%
%%DATA
%%%%long term
ydata = xlsread('50nm split.xlsx','B2:B1202');
tdata = xlsread('50nm split.xlsx','A2:A1202');

%%%short term
%tdata=xlsread('50nm 4s.xlsx','A4:A43');
%ydata=xlsread('50nm 4s.xlsx','B4:B43');
%ydata = xlsread('150nm 4s.xlsx','B4:B43');
%ydata = xlsread('450nm 4s.xlsx','B4:B43');
%%%%%%%%%%%%%%%%%
%solve ODEs
options = odeset('RelTol',1e-6);%,'MaxOrder','1','BDF','on');
Xo=[initN;initNC;75;0;0;10000;0;0;0;0;0;0;0;0;0;0;0;0;0;0;initC;];
%Xo=[0;ini_n;75;0;0;10000;0;0;0;0;0;0;0;0;0;0;0;0;0;0;];
tspan=tdata;
[t,X]=ode23s(@p53ode,tspan,Xo,options,c1,c2,c3,c4,c5,c6,c7,c8,c9,c10,c11,...
    c12,c13,c14,c15,c16,c17,c18,c19,c20,c21,c22,c23,c24,c25,c26,c27);
%%%%%%%%%%%%%%%%%
%plot
%% normalize data
```

```
%ynorm=ydata./max(ydata);
%simnorm=X(:,13)./max(X(:,13));
%plot(tdata,ynorm,'ok',t,simnorm,'r','LineWidth',2);
%% use gain
%ygain=3.041357255478377e+06.*X(:,13);  %50 nM long term
%ygain=5.3513e+06.*X(:,13);  %50 nM short term
%ygain=6.7415e+06.*X(:,13);  %150 nM
%ygain=6.5734e+06.*X(:,13);  %450 nM
%plot(tdata,ydata,'ok','LineWidth',2);
%hold on
%plot(t,ygain,'r','LineWidth',2);
%% plot options
set(gca,'FontSize',12,'FontName','Arial');
xlabel('Time (s)');ylabel('RLU');
%% plot individual portions of ODE
%subplot(4,3,1);plot(t,X(:,4),'m','LineWidth',2);title('nca'); subplot...
    (4,3,2);plot(t,X(:,5),'m','LineWidth',2);title('cnl');
%subplot(4,3,3);plot(t,X(:,7),'m','LineWidth',2);title('ncla');  subplot...
    (4,3,4);plot(t,X(:,8),'m','LineWidth',2);title('ncLA');
%subplot(4,3,5);plot(t,X(:,17),'m','LineWidth',2);title('nla');  subplot...
    (4,3,6);plot(t,X(:,18),'m','LineWidth',2);title('nLA');
%subplot(4,3,7);plot(t,X(:,5),'m','LineWidth',2);title('cna');  subplot...
    (4,3,8);plot(t,X(:,5),'m','LineWidth',2);title('CNl');
%subplot(4,3,9);plot(t,X(:,10),'m','LineWidth',2);title('Noxy'); subplot...
    (4,3,10);plot(t,X(:,14),'m','LineWidth',2);title('oxy');
%subplot(4,3,11); plot(t,X(:,13),'m','LineWidth',2);title('light');%...
    subplot(4,3,12); plot(tdata,ydata);
return
%%%%%%%%%%%%%%%%%%%%%%%%%%%%%%%%%%%
function init=plot_KDp(Q)        %function to solve initial conditions
options = odeset('RelTol',1e-6);
initN=Q(1);initC=Q(6);initNC=0;
kd=Q(2);cr=Q(3);cf=cr/kd;deg=Q(4);
Xo=[initN;initC;initNC;];
if Q(5) == 0  %no incubation
       init=[Q(1);Q(6);0;];  %return provided initial conditions
       return
end
tend=Q(5);
tspan=0:tend;
[t,X]=ode15s(@odeKD,tspan,Xo,options,cf,cr,deg);
%% plot initial conditions
%plot(t,X(:,1),t,X(:,3),'Linewidth',2);
%set(gca,'FontSize',12,'FontName','Arial');
%legend('[N]','[NC]');xlabel('Time (s)');ylabel('Concentration (uM)');
A=X(tend,1);
B=X(tend,3);
C=X(tend,2);
init=[A;B;C;];
return
%%%%%%%%%%%%%%%%%%%%%%%%%%%%%%%%%%%
function[dx_dt]=odeKD(t,x,cf,cr,deg)        %%ODE for initial conditions
dx_dt(1)=-cf.*x(1).*x(2)+cr.*x(3)-deg.*x(1);
dx_dt(2)=-cf.*x(1).*x(2)+cr.*x(3)-deg.*x(2);
```

```
149 dx_dt(3)=cf.*x(1).*x(2)-cr.*x(3)-deg.*x(3);
150 dx_dt=dx_dt';
151 return
152 %%%%%%%%%%%%%%%%%%%%%%%%%%%%%%%%%%%%
153 function[dx_dt]=p53ode(t,x,c1,c2,c3,c4,c5,c6,c7,c8,c9,c10,c11,c12,c13,c14,...
      c15,c16,c17,c18,c19,c20,c21,c22,c23,c24,c25,c26,c27)
154 %ODE
155 dx_dt(1)=-c1.*x(1).*x(21)+c2.*x(2)-c9.*x(1).*x(6)+c10.*x(16)-c7.*x(1).*x...
      (3)+c8.*x(15)-c24.*x(1).*x(14)+c25.*x(19)-c26.*x(1).*x(12)+c27.*x(20)-...
      c15.*x(1).*x(9)+c16.*x(18);
156 dx_dt(2)=c1.*x(1).*x(21)-c2.*x(2)-c3.*x(2).*x(3)+c4.*x(4)-c5.*x(2).*x(6)+...
      c6.*x(5)-c21.*x(2).*x(12)+c22.*x(11)-c19.*x(2).*x(14)+c20.*x(10)-c15.*...
      x(2).*x(9)+c16.*x(8);
157 dx_dt(3)=-c3.*x(2).*x(3)+c4.*x(4)-c3.*x(5).*x(3)+c4.*x(7)-c7.*x(1).*x(3)+...
      c8.*x(15)-c7.*x(16).*x(3)+c8.*x(17);
158 dx_dt(4)=c3.*x(2).*x(3)-c4.*x(4)-c5.*x(4).*x(6)+c6.*x(7)+c1.*x(15).*x(21)-...
      c2.*x(4);
159 dx_dt(5)=-c3.*x(5).*x(3)+c4.*x(7)+c5.*x(2).*x(6)-c6.*x(5)+c1.*x(16).*x(21)...
      -c2.*x(5);
160 dx_dt(6)=-c5.*x(2).*x(6)+c6.*x(5)-c5.*x(4).*x(6)+c6.*x(7)-c9.*x(1).*x(6)+...
      c10.*x(16)-c9.*x(15).*x(6)+c10.*x(17);
161 dx_dt(7)=c3.*x(5).*x(3)-c4.*x(7)+c5.*x(4).*x(6)-c6.*x(7)+c1.*x(17).*x(21)-...
      c2.*x(7)-c11.*x(7)+c12.*x(8);
162 dx_dt(8)=c11.*x(7)-c12.*x(8)+c1.*x(18).*x(21)-c2.*x(8)-c18.*x(8)+c15.*x(2)...
      .*x(9)-c16.*x(8);
163 dx_dt(9)=-c15.*x(2).*x(9)+c16.*x(8)-c15.*x(1).*x(9)+c16.*x(18);
164 dx_dt(10)=c18.*x(8).*(1-c23)+c1.*x(19).*x(21)-c2.*x(10)+c19.*x(2).*x(14)-...
      c20.*x(10);
165 dx_dt(11)=c18.*c23.*x(8)+c1.*x(20).*x(21)-c2.*x(11)+c21.*x(2).*x(12)-c22.*...
      x(11);
166 dx_dt(12)=-c21.*x(2).*x(12)+c22.*x(11)-c26.*x(1).*x(12)+c27.*x(20);
167 dx_dt(13)=c18.*x(8).*(1-c23)-x(13)+c17.*x(18).*(1-c23);
168 dx_dt(14)=-c19.*x(2).*x(14)+c20.*x(10)-c24.*x(1).*x(14)+c25.*x(19);
169 dx_dt(15)=c7.*x(1).*x(3)-c8.*x(15)-c9.*x(15).*x(6)+c10.*x(17)-c1.*x(15).*x...
      (21)+c2.*x(4);
170 dx_dt(16)=c9.*x(1).*x(6)-c10.*x(16)-c7.*x(16).*x(3)+c8.*x(17)-c1.*x(16).*x...
      (21)+c2.*x(5);
171 dx_dt(17)=-c13.*x(17)+c14.*x(18)+c9.*x(15).*x(6)-c10.*x(17)+c7.*x(16).*x...
      (3)-c8.*x(17)-c1.*x(17).*x(21)+c2.*x(7);
172 dx_dt(18)=c13.*x(17)-c14.*x(18)-c1.*x(18).*x(21)+c2.*x(8)-c17.*x(18)+c15.*...
      x(1).*x(9)-c16.*x(18);
173 dx_dt(19)=c17.*(1-c23).*x(18)-c1.*x(19).*x(21)+c2.*x(10)+c24.*x(1).*x(14)-...
      c25.*x(19);
174 dx_dt(20)=c17.*c23.*x(18)-c1.*x(20).*x(21)+c2.*x(11)+c26.*x(1).*x(12)-c27....
      *x(20);
175 dx_dt(21)=-c1.*x(21).*x(1)-c1.*x(21).*x(15)-c1.*x(21).*x(16)-c1.*x(21).*x...
      (17)-c1.*x(21).*x(20)-c1.*x(21).*x(19)+c2.*x(2)+c2.*x(4)+c2.*x(5)+c2.*...
      x(11)+c2.*x(10)+c2.*x(7)-c1.*x(21).*x(18)+c2.*x(8);
176 dx_dt=dx_dt';
177 return
```

Appendix B
Full Length Simulation

Fit to full length data Using the model, we can approximate the full length kinetics (Fig. B). Either because of the kinetics, or because of machine error, the data started out at the peak. To approximate this using the model, the affinity between the proteins fused to NFLuc and CFLuc was set to 0. The parameters were then altered to find the earliest peak, which occurred between 2-3 s. The model was simulated from 3 s onward, cutting off the peak. This simulation predicts that, relative to the NC complex, full length firefly luciferase has a higher affinity to L-oxy but a lower affinity to L-AMP, less dark reactions, and a moderately higher oxidation rate (Table B). Interestingly, improvements made in neither the adenylation rate nor the substrate affinity seems to affect the kinetics.

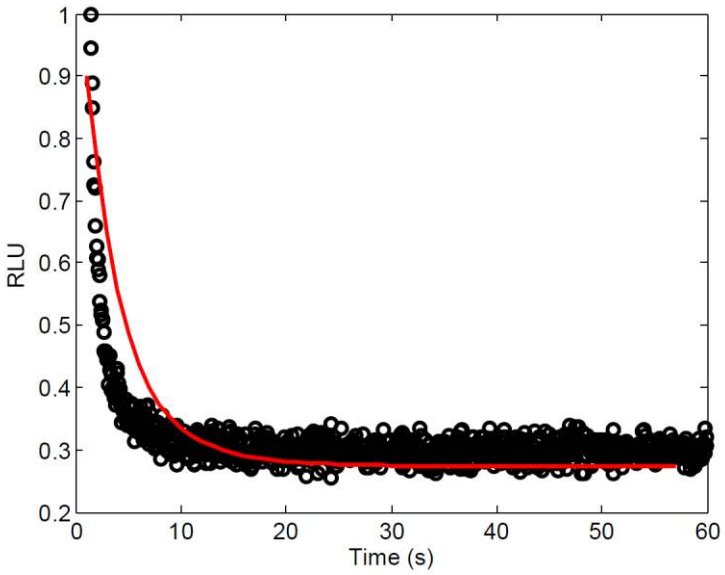

Figure B.1: Simulation of full length firefly luciferase kinetics using the FLCA model. By altering some of the parameters, the FLCA model can look like full length data.

Table B.1: Parameter Comparison

Parameter	NC complex	Full simulation	Full length (from [6])
Oxidation rate	0.22 s^{-1}	0.3 s^{-1}	0.167 s^{-1}
L-oxy affinity	70 nM	6 nM	500 nM
L-AMP affinity	460 pM	5.2 nM	3.8 nM
Dark reactions	0.2	0.29	0.2

Appendix C
Additional ODEs

ODE C1.

System of ODEs describing the interaction and degradation of two proteins.

$$\frac{dx_1}{dt} = -c_1 \cdot x_1 \cdot x_2 + c_2 \cdot x_3 - c_3 \cdot x_1$$
$$\frac{dx_2}{dt} = -c_1 \cdot x_1 \cdot x_2 + c_2 \cdot x_3 - c_3 \cdot x_2$$
$$\frac{dx_3}{dt} = c_1 \cdot x_1 \cdot x_2 - c_2 \cdot x_3 - c_3 \cdot x_3$$

Key to ODE C1

c_1	k_{on}
c_2	k_{off}
c_3	degradation
x_1	NFLuc
x_2	CFLuc
x_3	NC complex

ODE C2

Equations describing the binding of an inhibitor to a protein bound to CFLuc.

$$\frac{dx_{21}}{dt} = ... - c_{25} \cdot x_{21} \cdot x_{22} + c_{26} \cdot x_{23}$$
$$\frac{dx_{22}}{dt} = -c_{25} \cdot x_{21} \cdot x_{22} + c_{26} \cdot x_{23}$$
$$\frac{dx_{23}}{dt} = c_{25} \cdot x_{21} \cdot x_{22} - c_{26} \cdot x_{23}$$

Key to ODE C2

c_{25}	K_i forward
c_{26}	K_i reverse
x_{21}	CFLuc
x_{22}	Free inhibitor
x_{23}	CFLuc-Inhibitor complex

ODE C3.

Equations describing the interaction between two proteins and one inhibitor.

$$\frac{dx_1}{dt} = -c_1 \cdot x_1 \cdot x_2 + c_2 \cdot x_3$$
$$\frac{dx_2}{dt} = -c_1 \cdot x_1 \cdot x_2 + c_2 \cdot x_3 - c_3 \cdot x_4 \cdot x_2 + c_4 \cdot x_5$$
$$\frac{dx_3}{dt} = c_1 \cdot x_1 \cdot x_2 - c_2 \cdot x_3$$
$$\frac{dx_4}{dt} = -c_3 \cdot x_4 \cdot x_2 + c_4 \cdot x_5$$
$$\frac{dx_5}{dt} = c_3 \cdot x_4 \cdot x_2 - c_4 \cdot x_5$$

Key to ODE C3

c_1	k_{on}
c_2	k_{off}
c_3	K_i forward
c_4	K_i reverse
x_1	NFLuc
x_2	CFLuc
x_3	NC complex
x_4	Free inhibitor
x_5	CFLuc-inhibitor complex

Appendix D
Material and Methods for the FLCA

Measurement of the kinetics of *in vitro* FLCA Kinetic data of luminescence production in FLCA was obtained by our collaborators under the same conditions as previously published in [28]. Briefly, purified recombinant protein of p53 and mdm2 fused to NFLuc and CFLuc (50 nM) were suspended in a 2x enzyme solution containing 100 mM MOPS, 10 mM $MgSO_4$, pH 7.3. The mixture (50 μl) was dispensed to a well in a white 96-well plate (Corning-Costar, NY, USA) after incubation at 37°C for 120 s. The light intensity was measured immediately after injection of 50 μl 2x substrate solution (40 mM ATP and 150 μM LH_2 in 100 mM MOPS, 10 mM $MgSO_4$, pH 7.3) with a periodical integration for 0.1 s using Phelios AB-2350 luminometer (ATTO, Tokyo, Japan).

Vita

Renee Dale received her bachelor's degrees in Biological Sciences and Philosophy from Louisiana State University in 2013. She will receive her master's degree in August 2015, and plans to work on her doctorate at LSU thereafter.